Coculture of two Developmental Stages of a Marine-derived *Aspergillus alliaceus* Results in the Production of the Cytotoxic Bianthrone Allianthrone A

P. E. Mandelare, D. A. Adpressa, E. N. Kaweesa,

L. N. Zakharov, S. Loesgen*****

Content:

	NMR Spectra	Page#
Figure S1	^{1}H of compound **1** in chloroform-*d*	S4
Figure S2	^{1}H-^{1}H COSY of compound **1** in chloroform-*d*	S5
Figure S3	^{1}H-^{13}C HSQC of compound **1** in chloroform-*d*	S6
Figure S4	^{1}H-^{13}C HMBC of compound **1** in chloroform-*d*, 8 Hz optimized	S7
Table S1	Chemical shifts for compounds **2** and **3** in chloroform-*d*	S8
Figure S5	^{1}H of compound **2** in chloroform-*d*	S9
Figure S6	Crystal structure of compound **2**	S10
Figure S7	^{1}H of compound **3** in chloroform-*d*	S11
Figure S8	^{1}H-^{1}H COSY of compound **3** in chloroform-*d*	S12
Figure S9	^{1}H-^{13}C HSQC of compound **3** in chloroform-*d*	S13
Figure S10	^{1}H-^{13}C HMBC of compound **3** in chloroform-*d*, 4 Hz optimized	S14
Figure S11	^{1}H-^{13}C HMBC of compound **3** in chloroform-*d*, 8 Hz optimized	S15
Figure S12	^{1}H of compound **4** in acetonitrile-d_3	S16
Figure S13	^{1}H of compound **4** in acetonitrile-d_3, 7.0 to 5.8 ppm expansion	S17
Figure S14	^{1}H of compound **4** in acetonitrile-d_3, 4.8 to 3.6 ppm expansion	S18
Figure S15	^{1}H of compound **4** in acetonitrile-d_3, 2.7 to 1.2 ppm expansion	S19
Figure S16	^{13}C of compound **4** in acetonitrile-d_3	S20
Figure S17	DEPT 135-^{13}C of compound **4** in acetone-d_3	S21
Figure S18	^{1}H-^{1}H COSY of compound **4** in acetone-d_3	S22

Figure S19	^{1}H-^{13}C HSQC of compound **4** in acetonitrile-d_3	S23
Figure S20	^{1}H-^{13}C HMBC of compound **4** in acetone-d_3, 4 Hz optimized	S24
Figure S21	^{1}H-^{13}C HMBC of compound **4** in acetone-d_3, 8 Hz optimized	S25
Figure S22	^{1}H-^{13}C HMBC of compound **4** in acetonitrile-d_3, 4 Hz optimized	S26
Figure S23	SEL-TOCSY of compound **4** in acetonitrile-d_3 of H-12	S27
Figure S24	SEL-TOCSY of compound **4** in acetonitrile-d_3 of H-11 and 12-OH	S28
Figure S25	SEL-TOCSY of compound **4** in acetonitrile-d_3 of H-13	S29
Figure S26	^{1}H of compound **5** in acetonitrile-d_3	S30
Figure S27	^{1}H of compound **6** in acetonitrile-d_3	S31
Figure S28	^{13}C of compound **5** in acetonitrile-d_3	S32
Figure S29	^{13}C of compound **6** in acetonitrile-d_3	S33
Figure S30	^{1}H-^{13}C HSQC of compound **5** in acetonitrile-d_3	S34
Figure S31	^{1}H-^{13}C HSQC of compound **6** in acetonitrile-d_3	S35
Figure S32	^{1}H-^{13}C HMBC of compound **5** in acetonitrile-d_3, 4 Hz optimized	S36
Figure S33	^{1}H-^{13}C HMBC of compound **6** in acetonitrile-d_3, 4 Hz optimized	S37
Figure S34	^{13}C-^{35}Cl/^{37}Cl isotope shift of compounds **4-6** in acetonitrile-d_3	S38
	Cell viability assay	
Figure S35	IC_{50} curve of compounds **4-6** against SK-Mel 5 cell lines	S39
Figure S36	IC_{50} curve of compounds **4-6** against HCT-116 cell lines	S40
Figure S37	IC_{50} curve of compounds **4-6** against A549 cell lines	S41
Figure S38	IC_{50} curve of compounds **4-6** against PC3 cell lines	S42
Figure S39	IC_{50} curve of compounds **4-6** against MCF7 cell lines	S43
	Antimicrobial assay	
Figure S40	Overall antimicrobial activity of compounds **1, 2,** and **4-6** in ethanol	S44
	***Aspergillus alliaceus* coculture study**	

Figure S41	Visual of coculture experiments with *A. alliaceus* phenotypes	S45
Figure S42	Metabolite comparison of *A. alliaceus* phenotypes via LC/MS analysis	S46
Figure S43	Metabolite production plot of induced *A. alliaceus* after coculture experiment	S47
Figure S44	Metabolite production plot of *A. alliaceus* phenotype coculture experiment	S48
Figure S45	Metabolite production plot of *A. alliaceus* (sclerotia-forming phenotype)	S49
Figure S46	Metabolite production plot of *A. alliaceus* (conidia-forming phenotype)	S50
Figure S47	Induction of conidia-forming *A. alliaceus* phenotype	S51
Figure S48	Induction of sclerotia-forming *A. alliaceus* phenotype	S52
	DNA taxonomy of *A. alliaceus* developmental stages	
Figure S49	Phylogenetic consensus tree of *A. alliaceus* phenotypes, Beta-Tubulin, CAM, ITS regions	S53
Figure S50	Consensus sequence of conidia-forming *A. alliaceus* Beta-Tubulin, CAM, ITS regions	S54
Figure S51	Consensus sequence of sclerotia-forming *A. alliaceus* Beta-Tubulin, CAM, ITS regions	S55
	Biosynthetic proposal of compounds 2-6 from *A. alliaceus*	
Figure S52	Abbreviated biosynthetic proposal of compounds **2-6**	S56
	References	S57

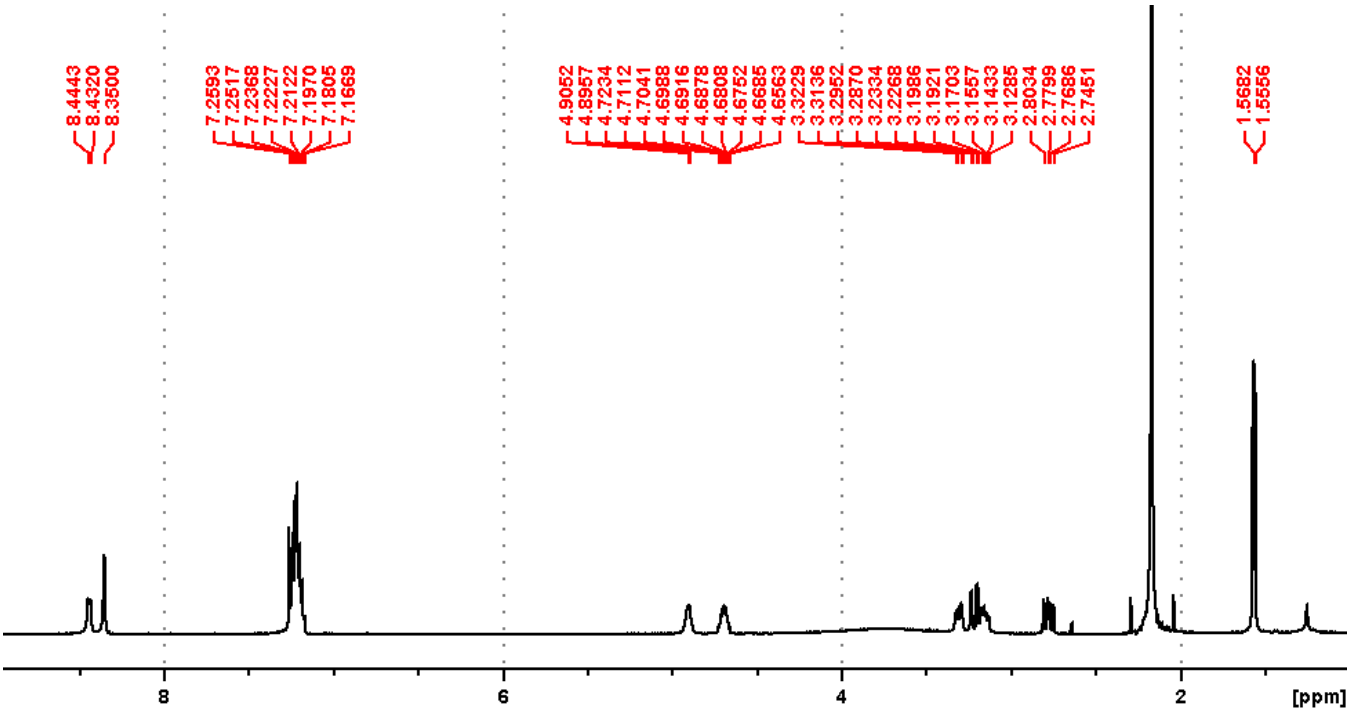

Figure S1: ^{1}H NMR of compound **1** in chloroform-*d* at 500 MHz.

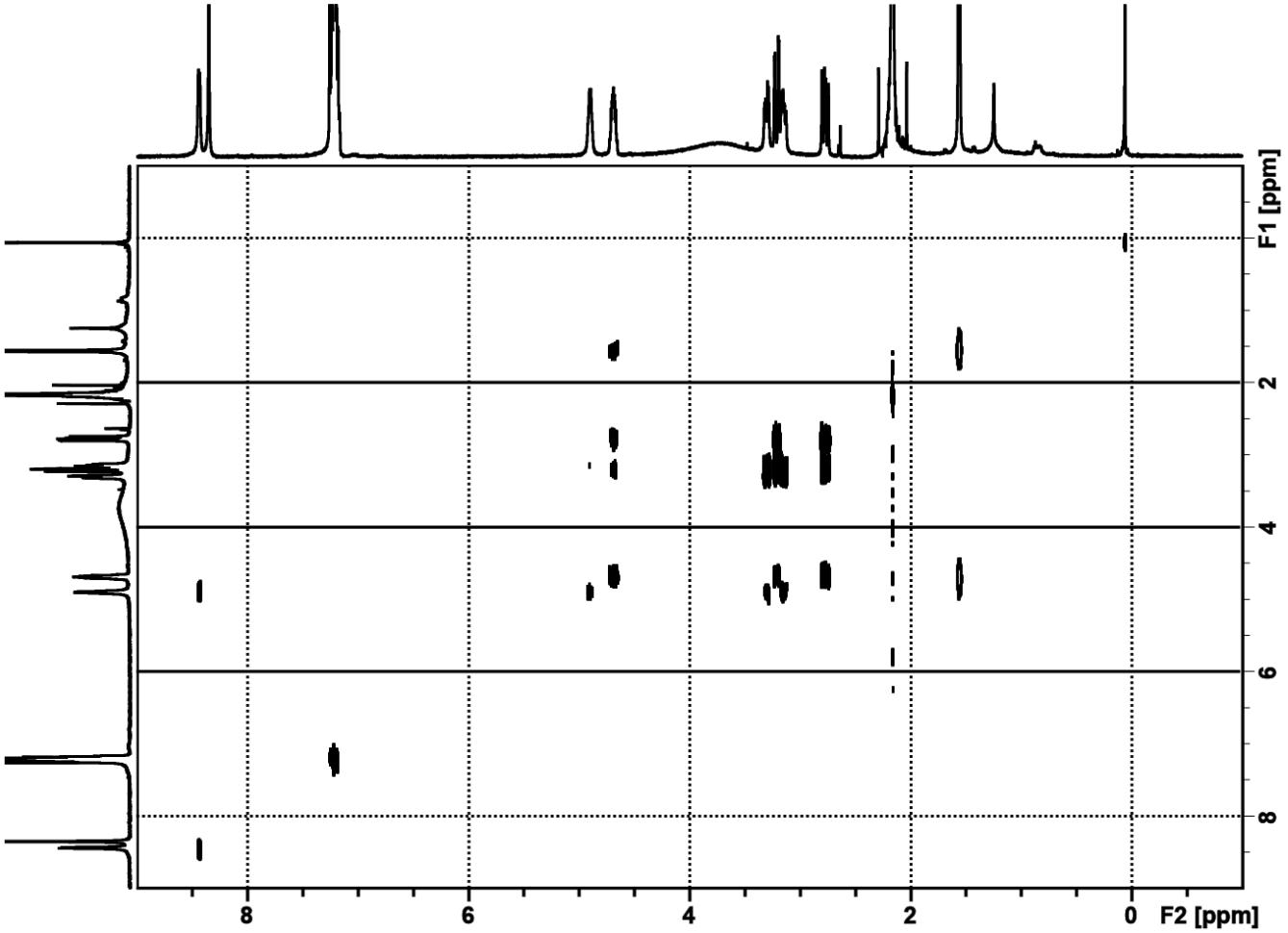

Figure S2: ^{1}H-^{1}H COSY NMR spectrum of compound **1** in chloroform-*d* at 500 MHz

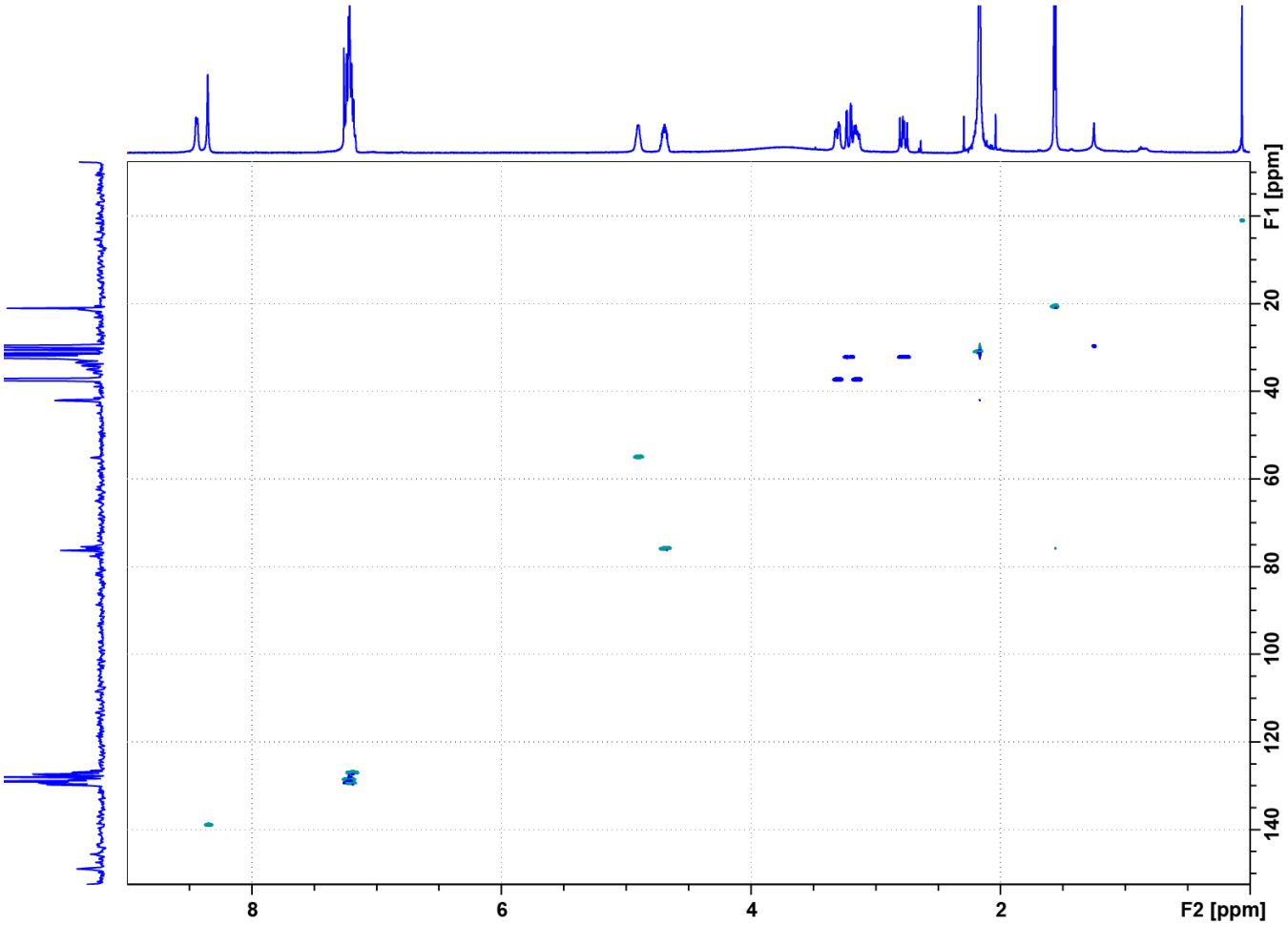

Figure S3: ^{1}H-^{13}C HSQC of compound **1** in chloroform-*d* at 500 MHz and 125 MHz

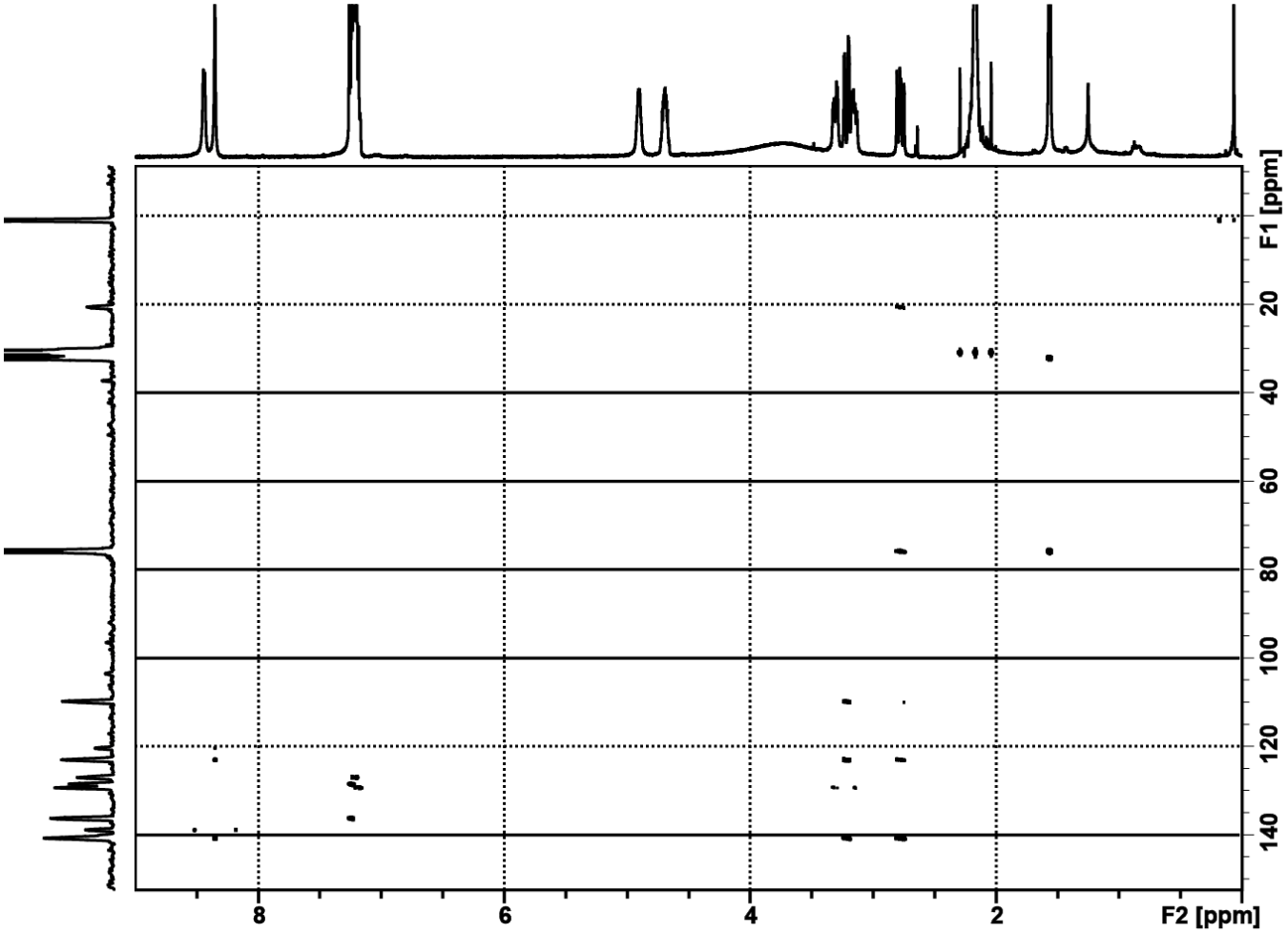

Figure S4: ^{1}H-^{13}C HMBC, 8 Hz optimized NMR spectrum of compound **1** in chloroform-*d* at 500 MHz and 125 MHz

Table S1: Compounds **2** and **3** ^{1}H and ^{13}C NMR Chemical Shifts in chloroform-*d* at 500 MHz and 125 MHz

	2	**3**	
position	δ_H (*J* in Hz)	δ_c, type	δ_H (*J* in Hz)
1		160.0, C	
1-OH	12.30, s		12.73, s
2	6.70, d (2.6)	111.1, C	
3		116.5, C	
4	7.38, d (2.5)	104.1, CH	7.47, s
4a		132.7, C	
5	7.69, d (1.6)	122.1., CH	7.70, d (1.6)
6		149.7, CH	
7	7.18, d (1.7)	125.5, CH	7.18, d (1.3)
8		162.7, C	
8-OH	12.14, s		11.95, s
8a		114.2, C	
9		181.3, C	
9a		114.2, C	
10		181.3, C	
10a		132.7, C	
11	2.86, dd (5.0, 5.1, 13.8); 2.82, d (7.2, 7.7, 13.8)	46.4, CH_2	2.85, dd (5.0, 5.4, 13.5); 2.63, dd (3.5, 7.7, 9.4)
12	4.15, m (5.2, 5.9, 6.1)	68.7, CH	4.17, m (5.4, 6.2)
13	1.29, d (6.1)	23.8, CH_3	1.30, d (6.2)
14-OCH_3	3.94, s	57.7, CH_3	4.11, s

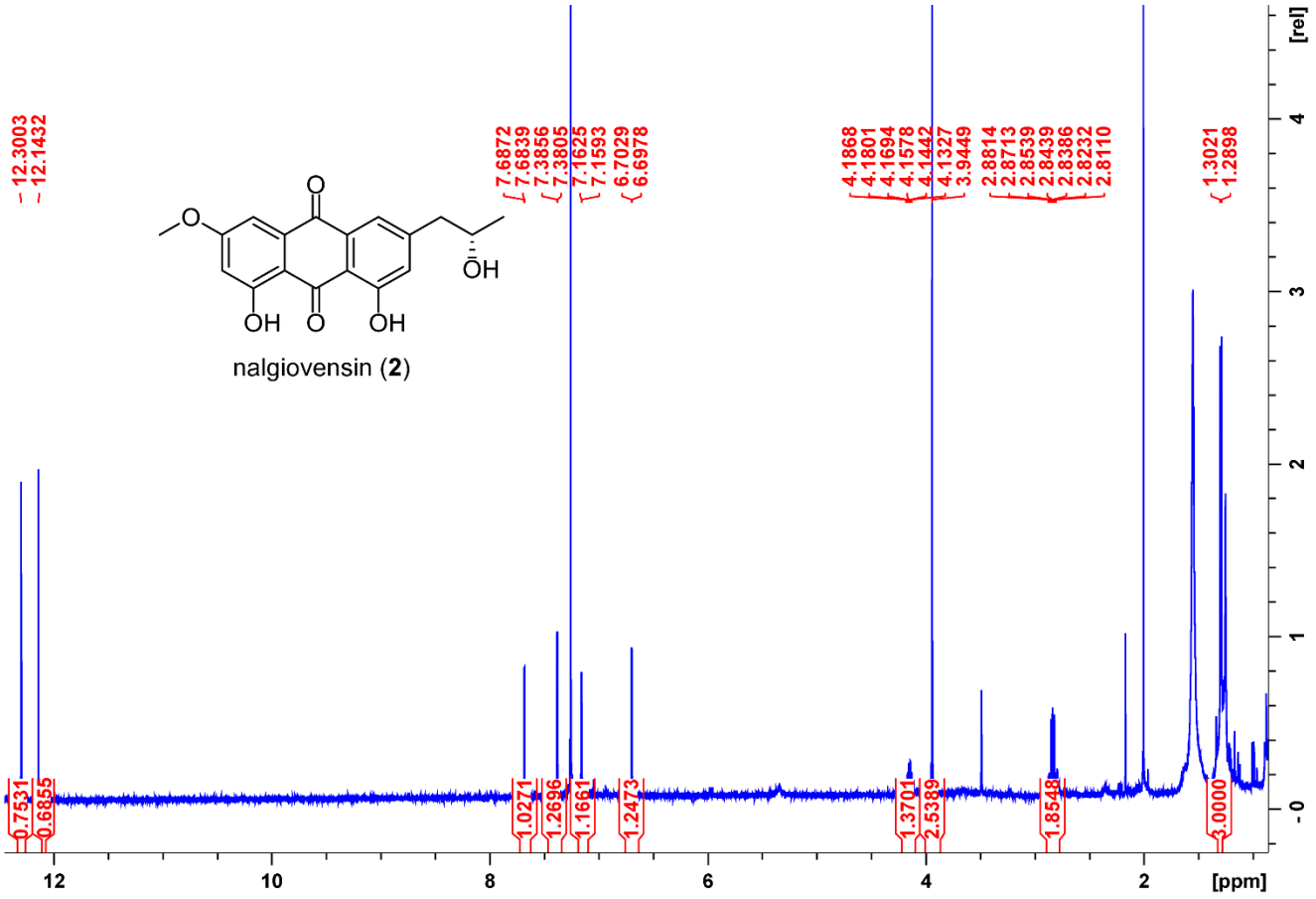

Figure S5: ^{1}H NMR spectrum of compound **2** in chloroform-*d* at 500 MHz

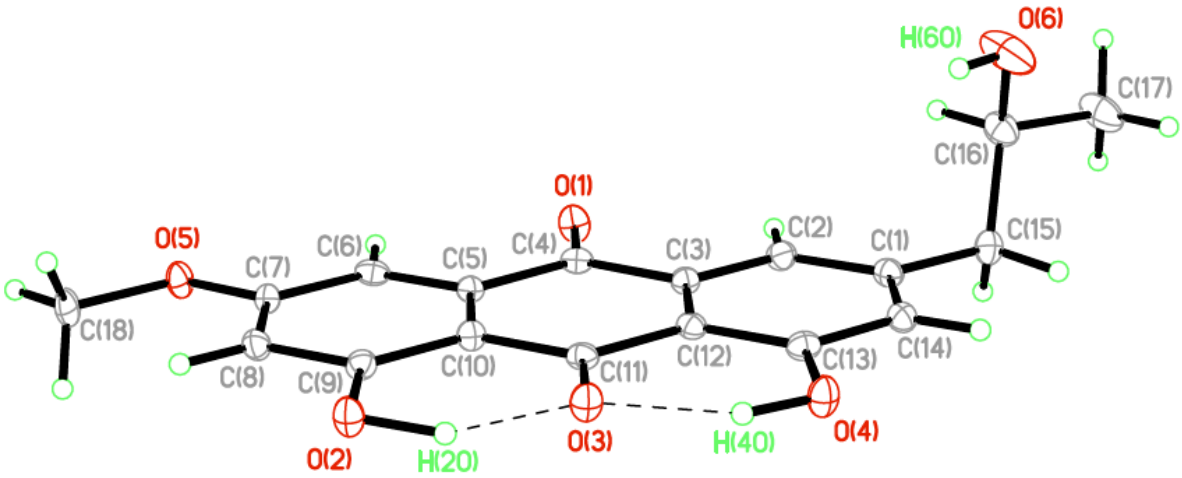

Figure S6: X-ray diffraction derived ORTEP plot of compound **2**. Compound **2** was dissolved in chloroform and placed in a vial with 50:50 methanol:water to create a crystal via solvent diffusion

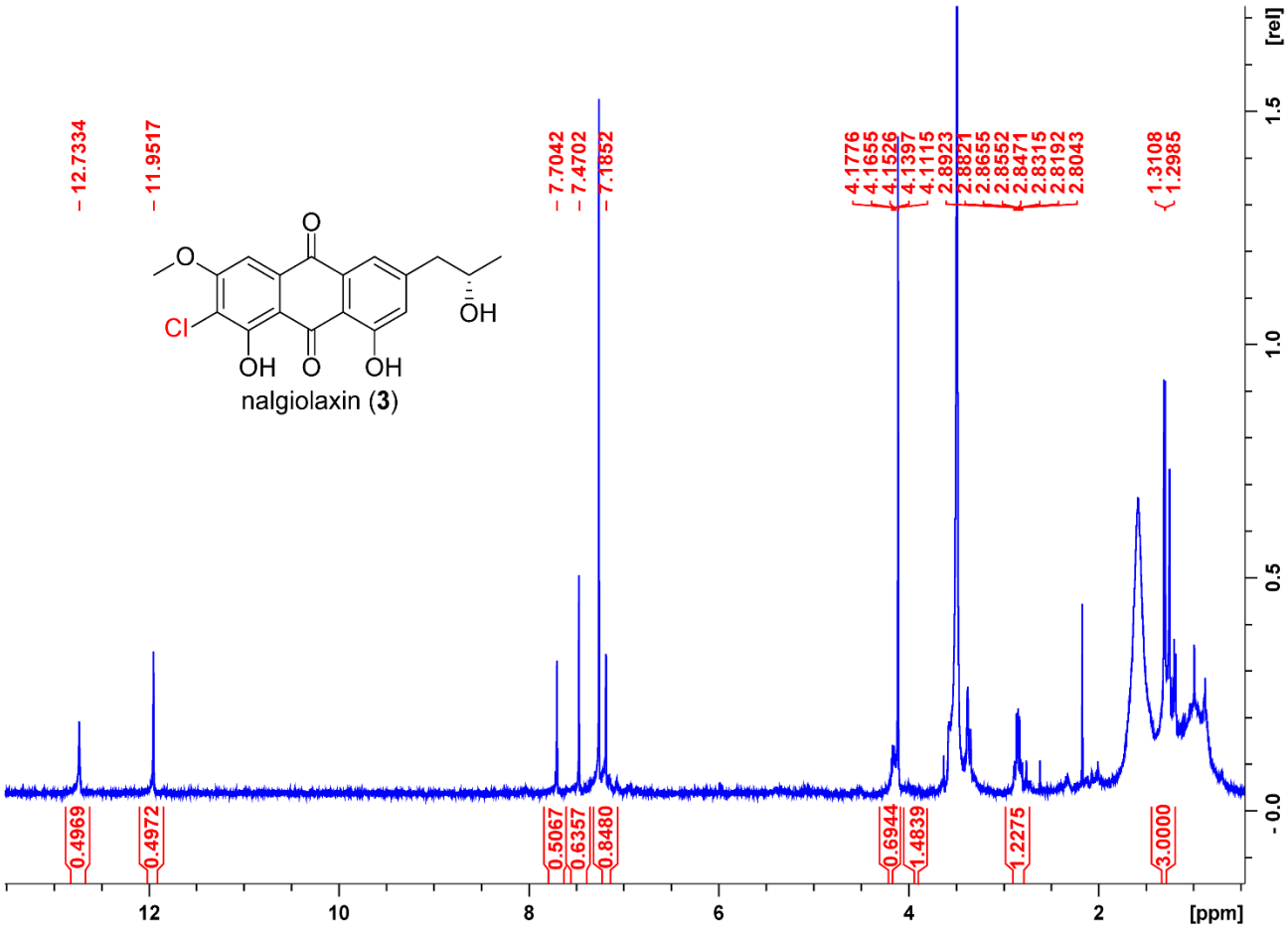

Figure S7: ^{1}H NMR spectrum of compound **3** in chloroform-*d* at 500 MHz

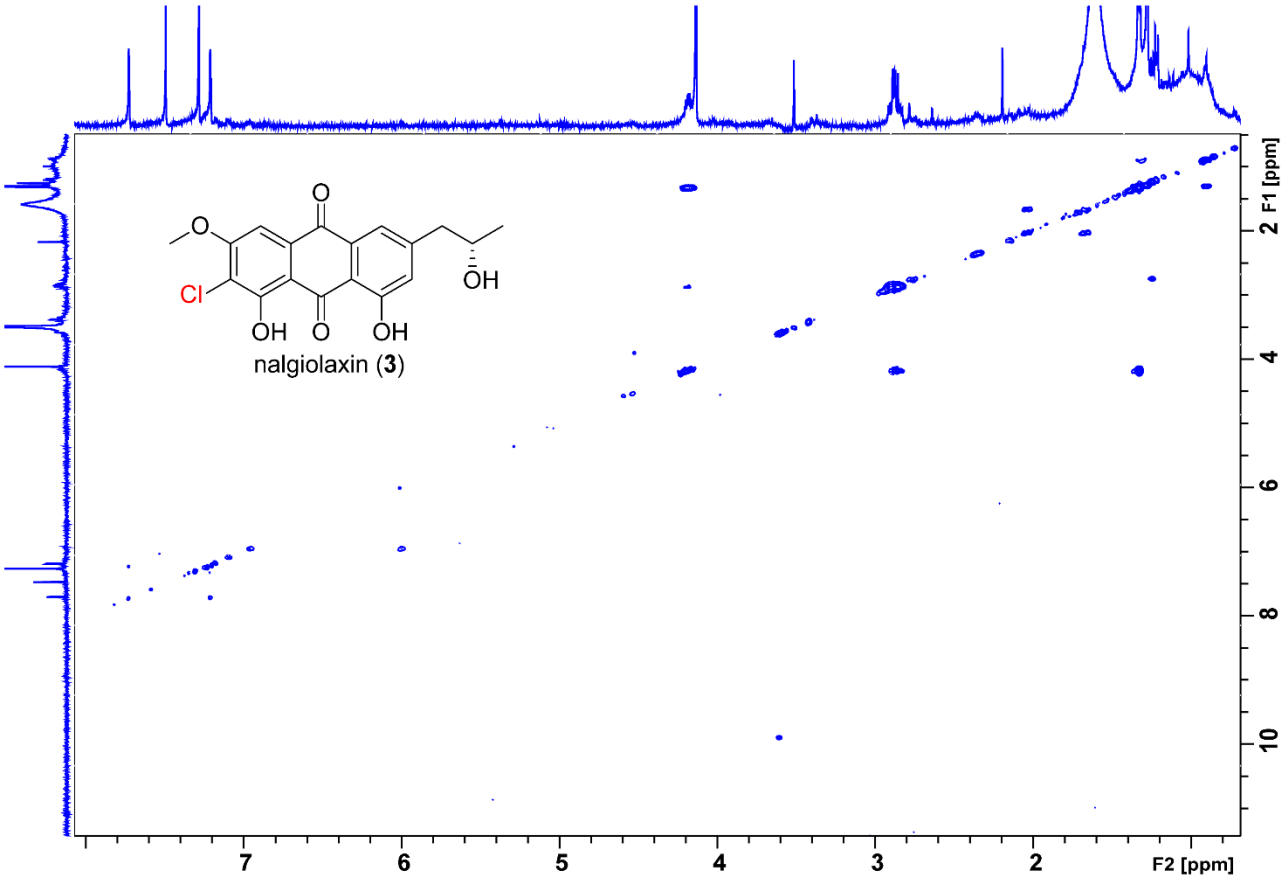

Figure S8: ^{1}H-^{1}H COSY NMR spectrum of compound **3** in chloroform-*d* at 500 MHz

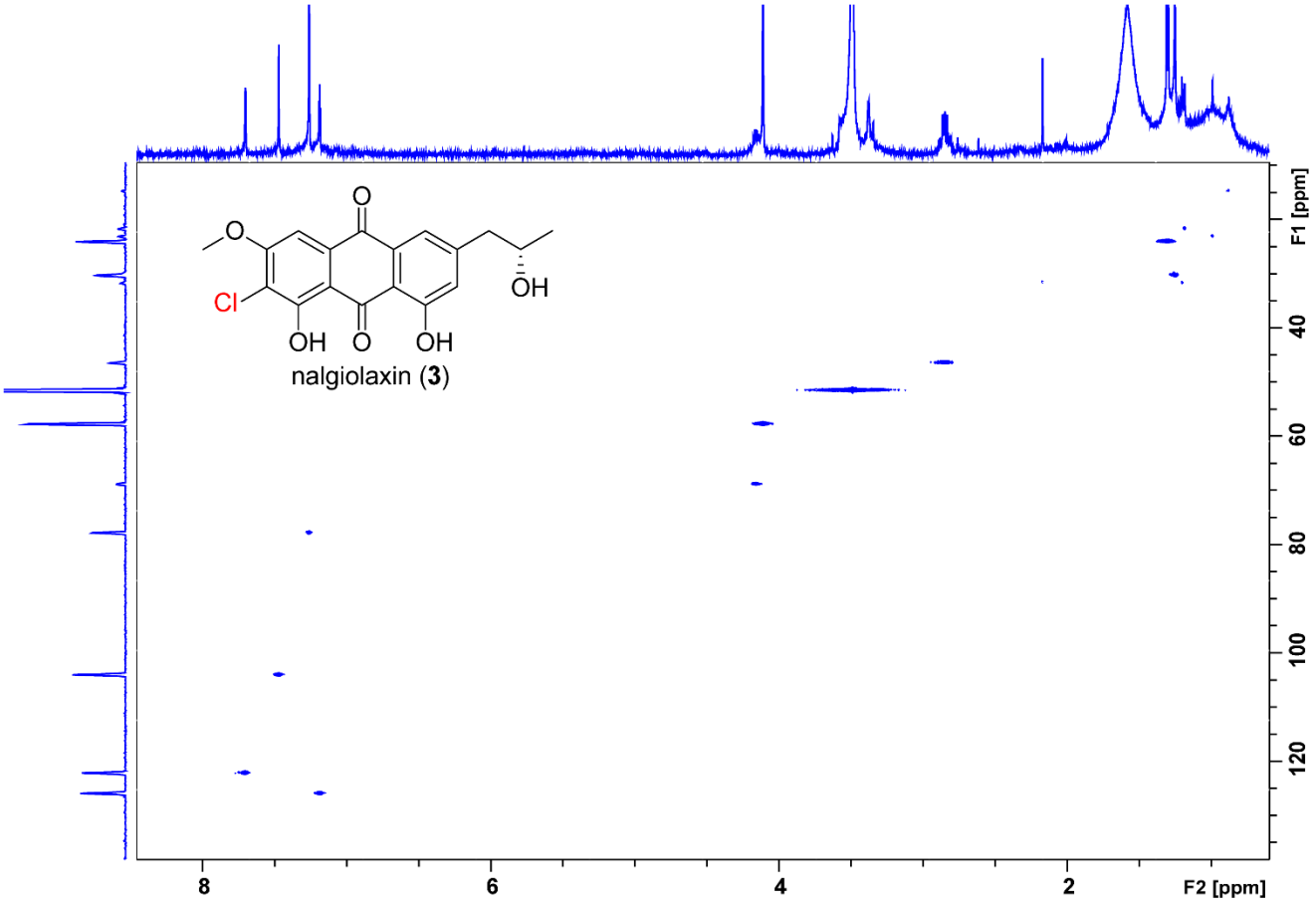

Figure S9: ^{1}H-^{13}C HSQC NMR spectrum of compound **3** in chloroform-*d* at 500 MHz and 125 MHz

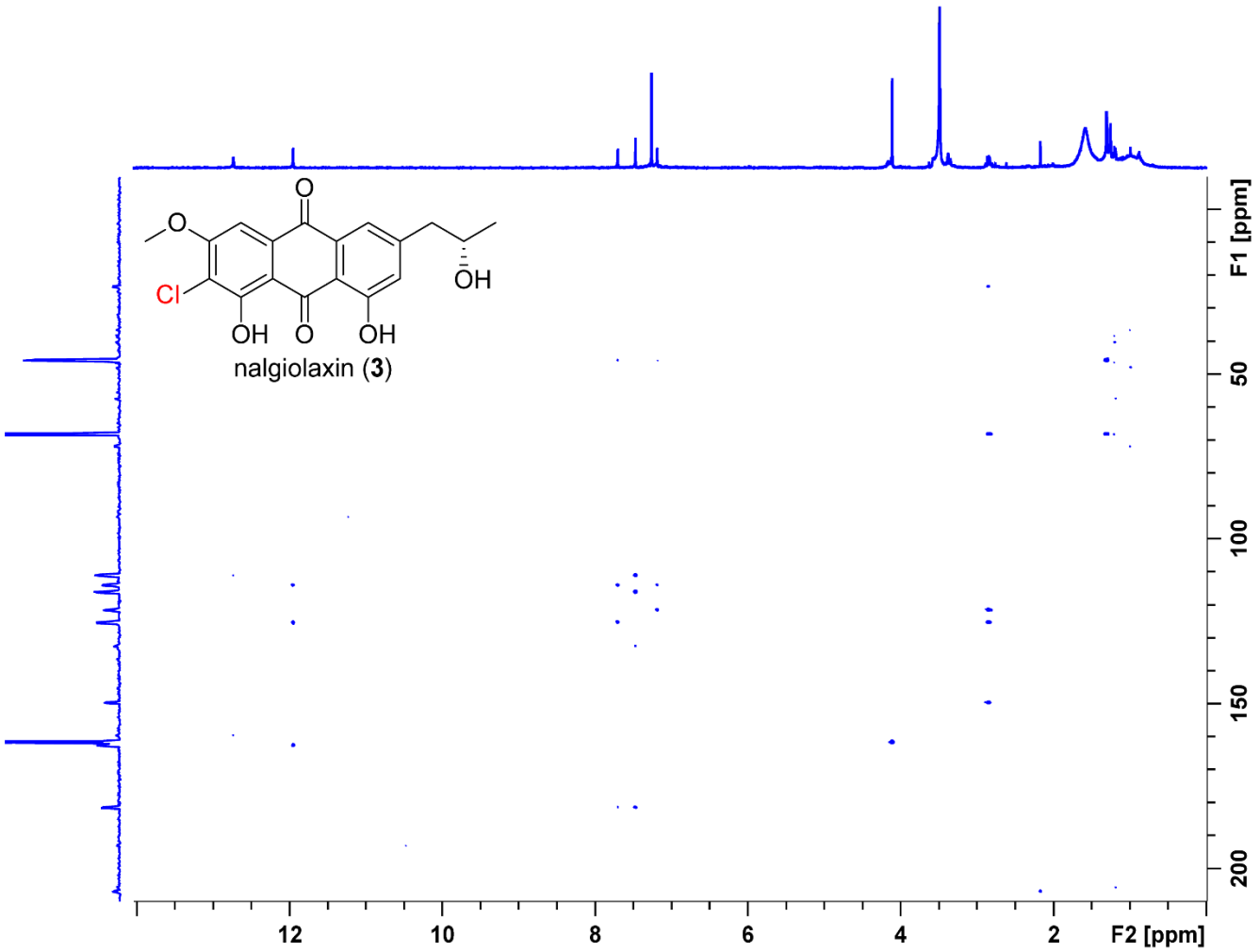

Figure S10: ^{1}H-^{13}C HMBC, 4 Hz optimized NMR spectrum of compound **3** in chloroform-*d* at 500 MHz and 125 MHz

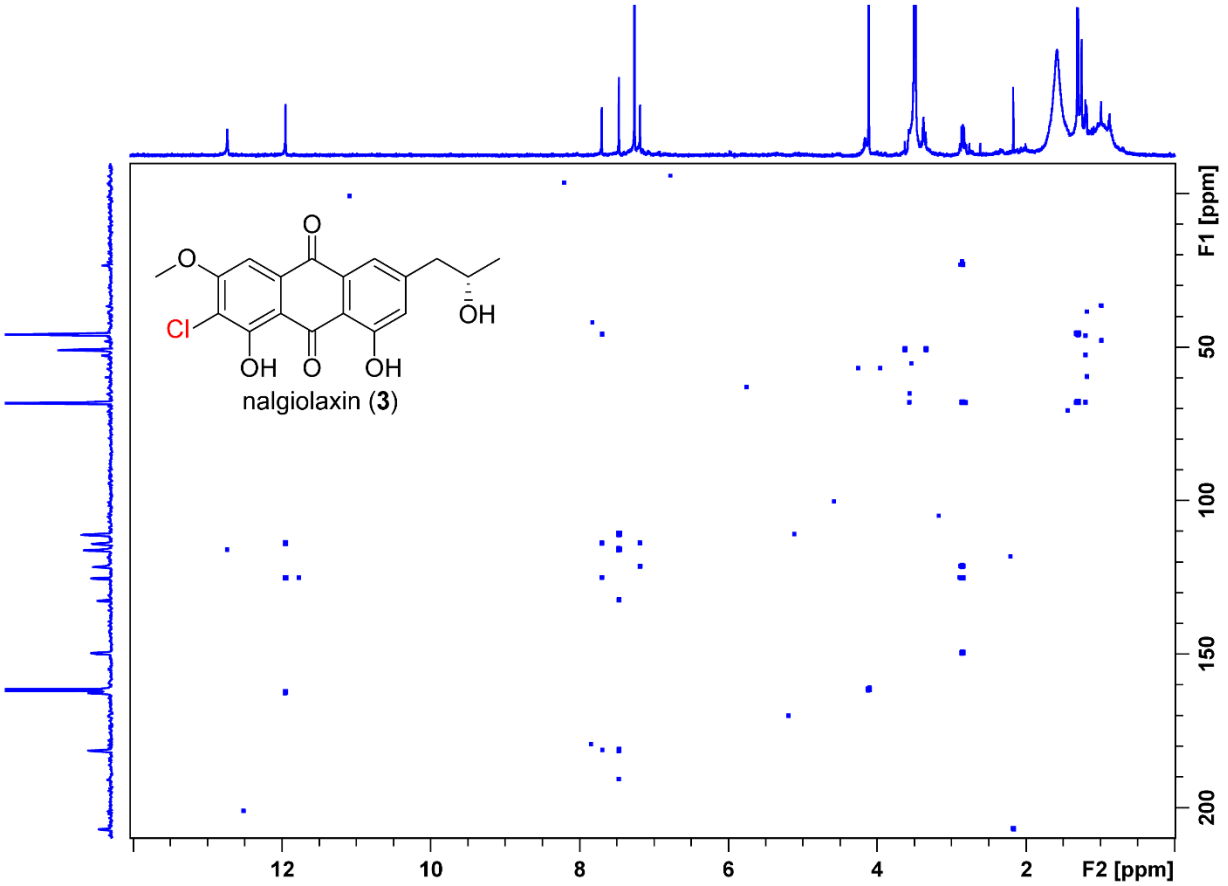

Figure S11: ^{1}H-^{13}C HMBC, 8 Hz optimized NMR spectrum of compound **3** in chloroform-*d* at 500 MHz and 125 MHz

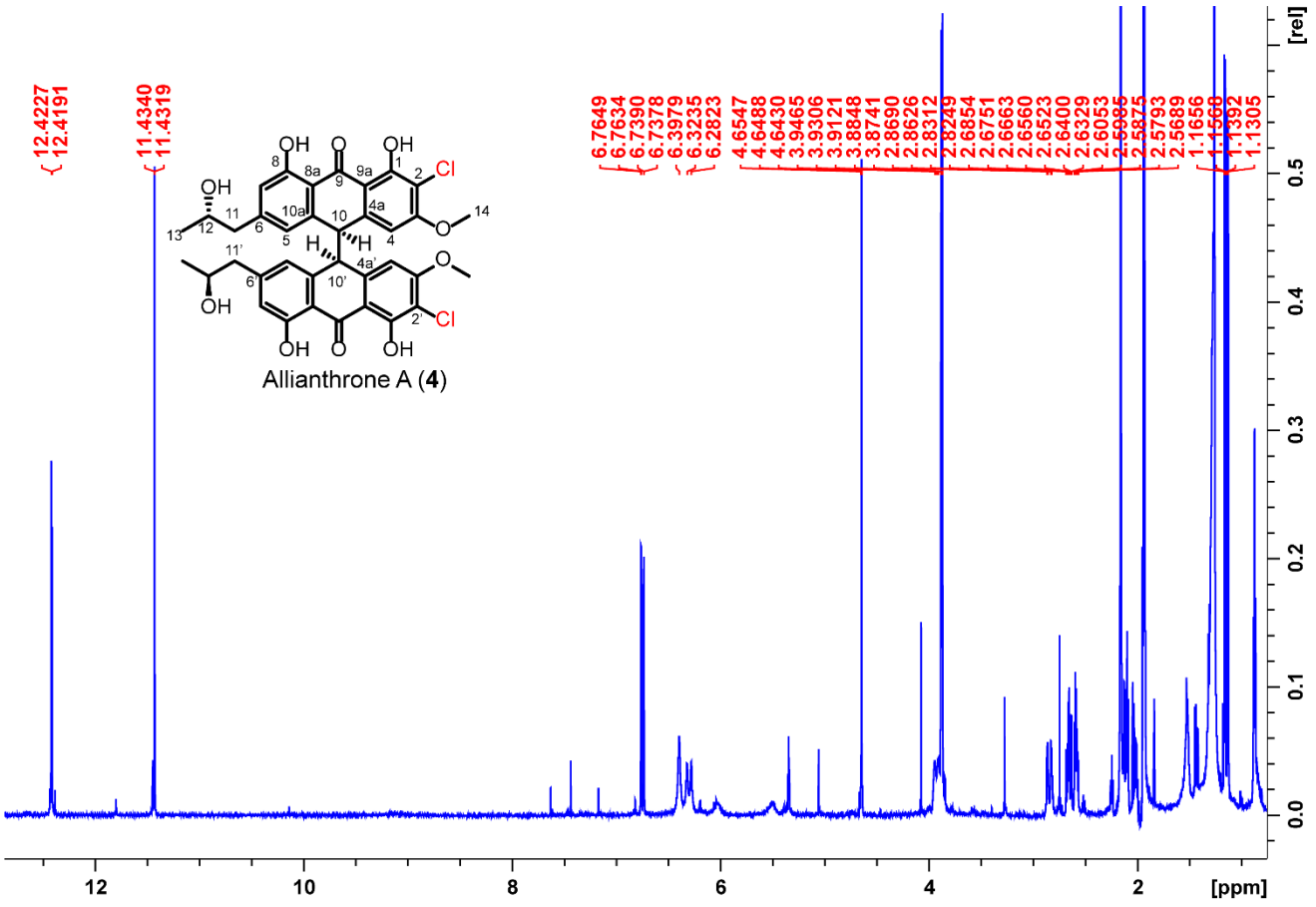

Figure S12: ^{1}H NMR spectrum of compound **4** in acetonitrile-d_3 at 700 MHz

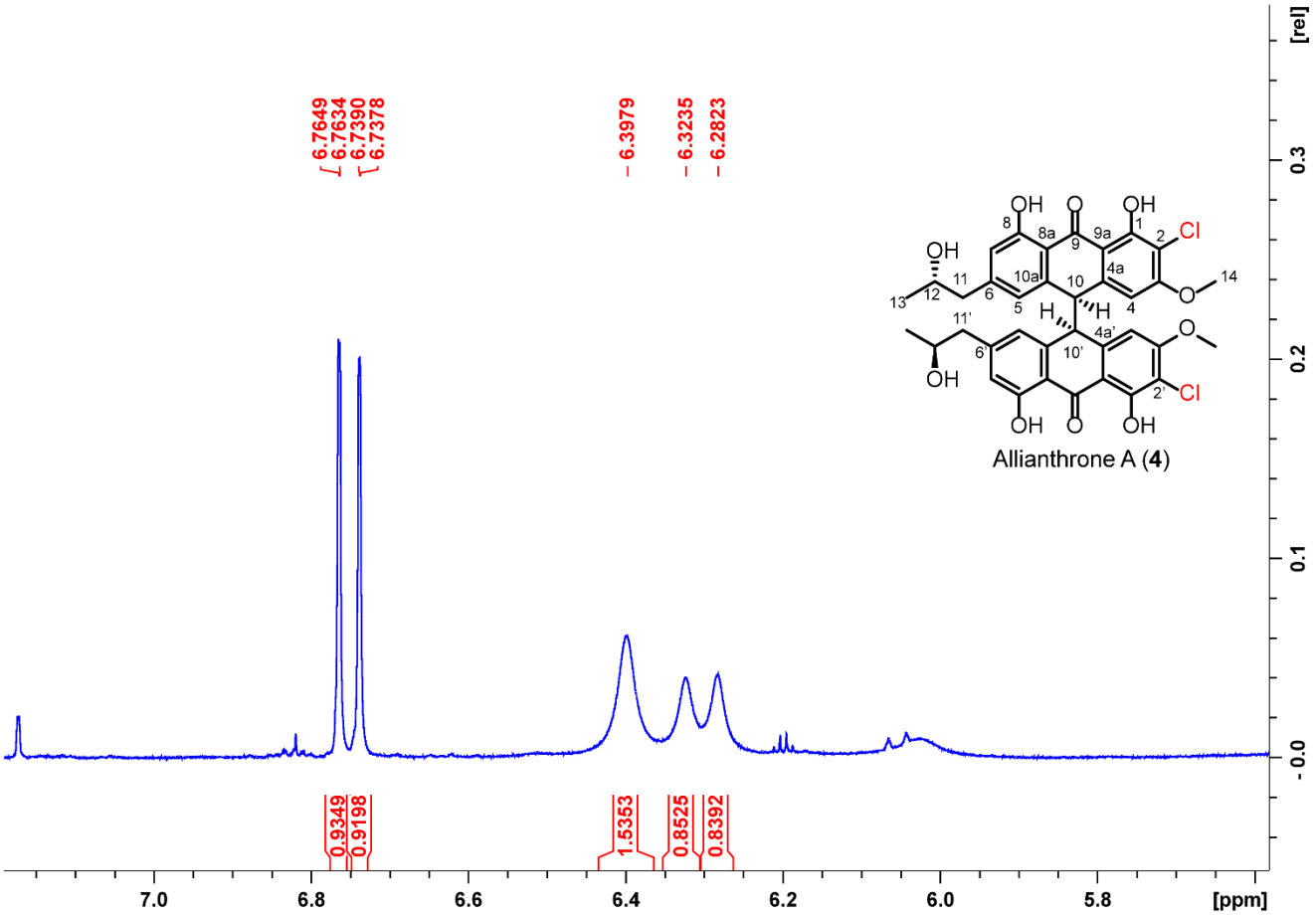

Figure S13: ^{1}H NMR spectrum, 7.0 to 5.8 ppm expansion, of compound **4** in acetonitrile-d_3 at 700 MHz

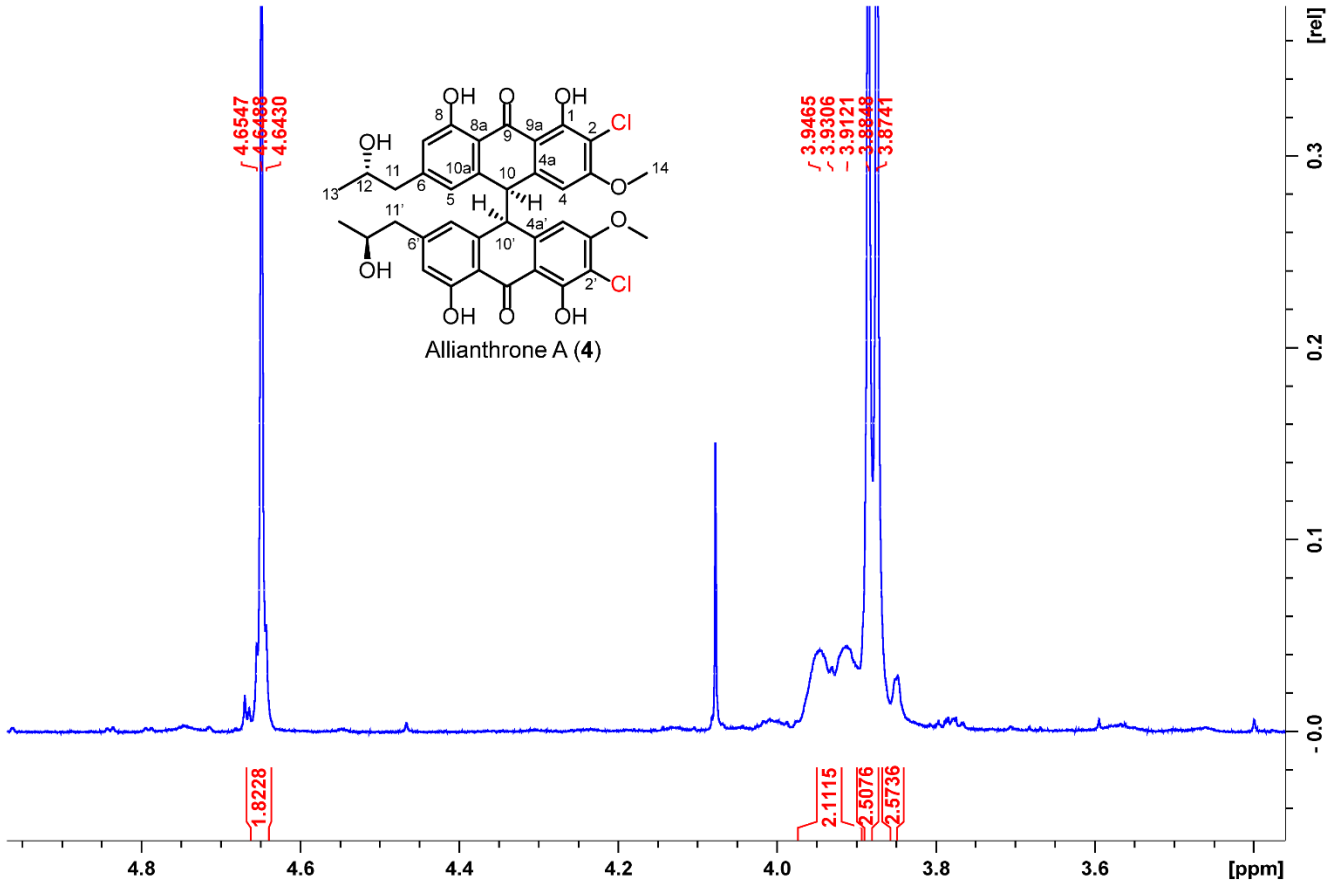

Figure S14: ^{1}H NMR spectrum, 4.8 to 3.6 ppm expansion, of compound **4** in acetonitrile-d_3 at 700 MHz

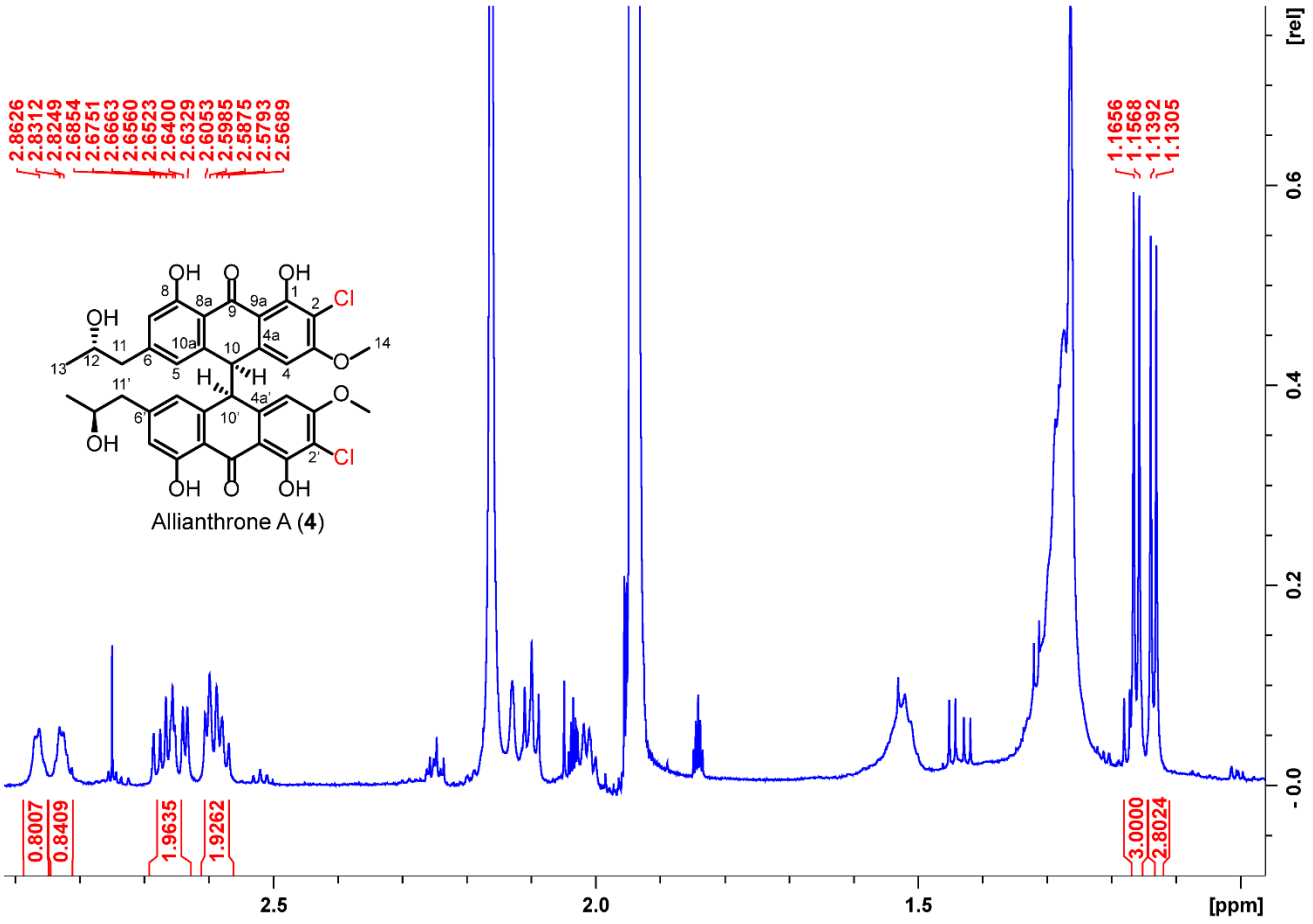

Figure S15: ^{1}H NMR spectrum, 2.7 to 1.2 ppm expansion, of compound **4** in acetonitrile-d_3 at 700 MHz

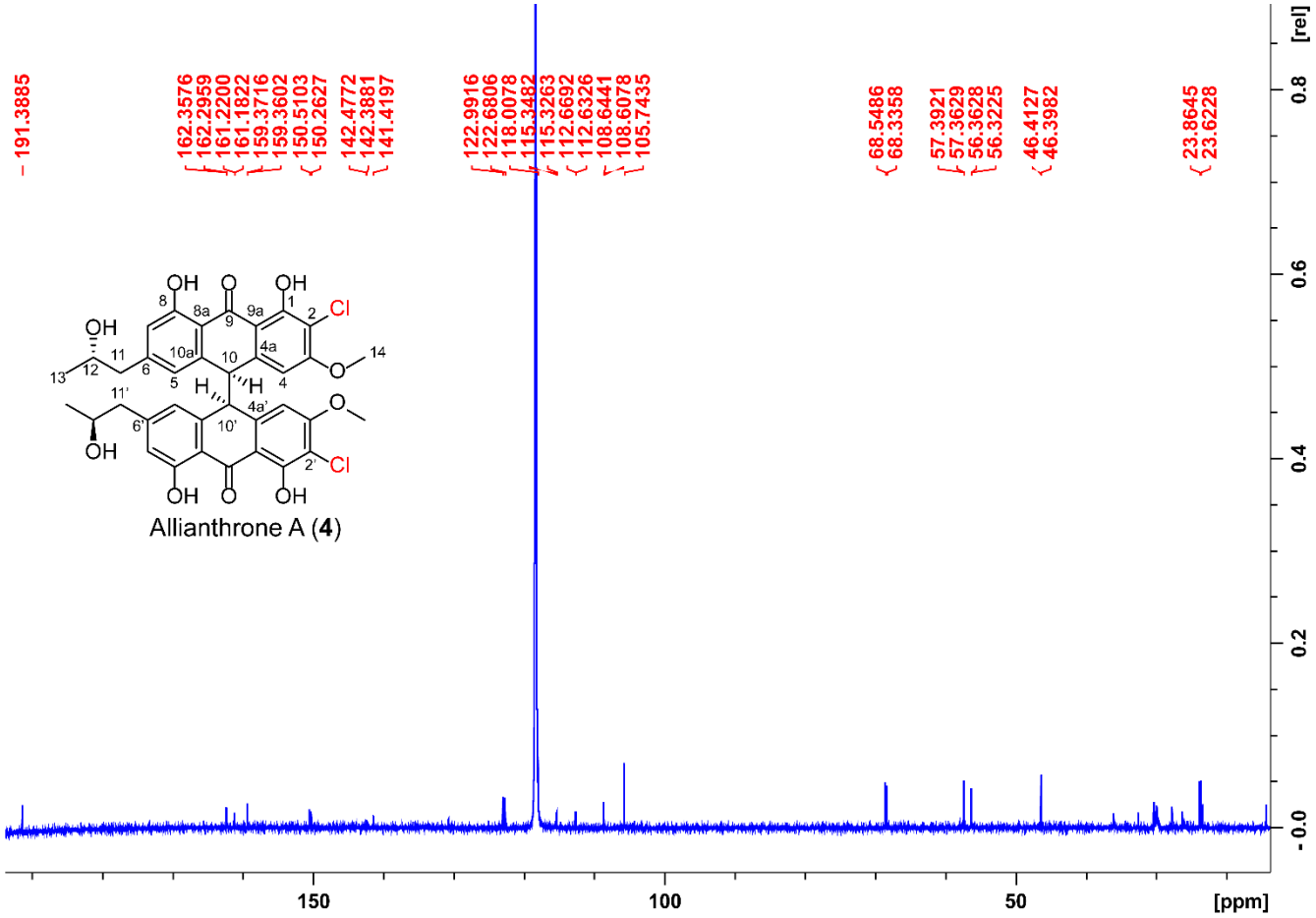

Figure S16: ^{13}C NMR spectrum of compound **4** in acetonitrile-d_3 at 176 MHz

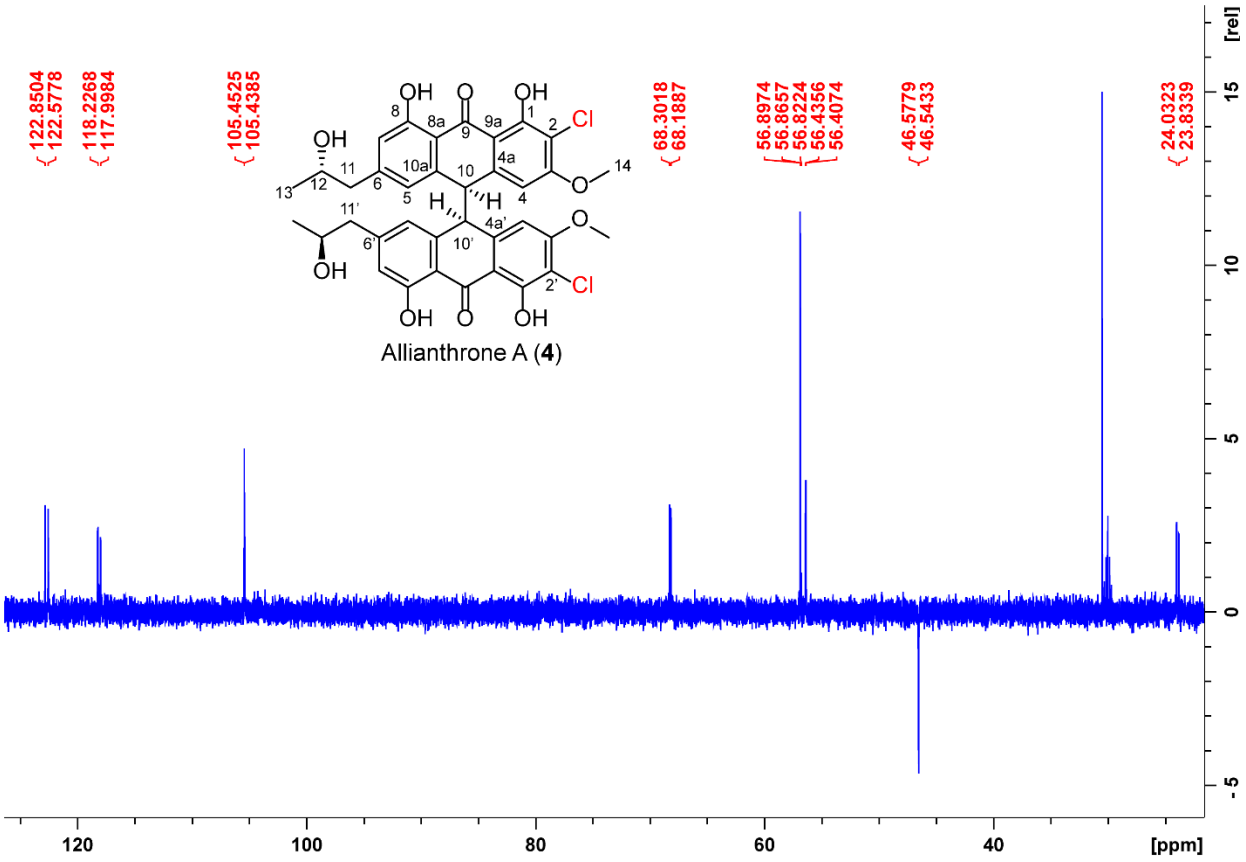

Figure S17: DEPT 135-^{13}C NMR spectrum of compound **4** in acetone-d_3 at 125 MHz

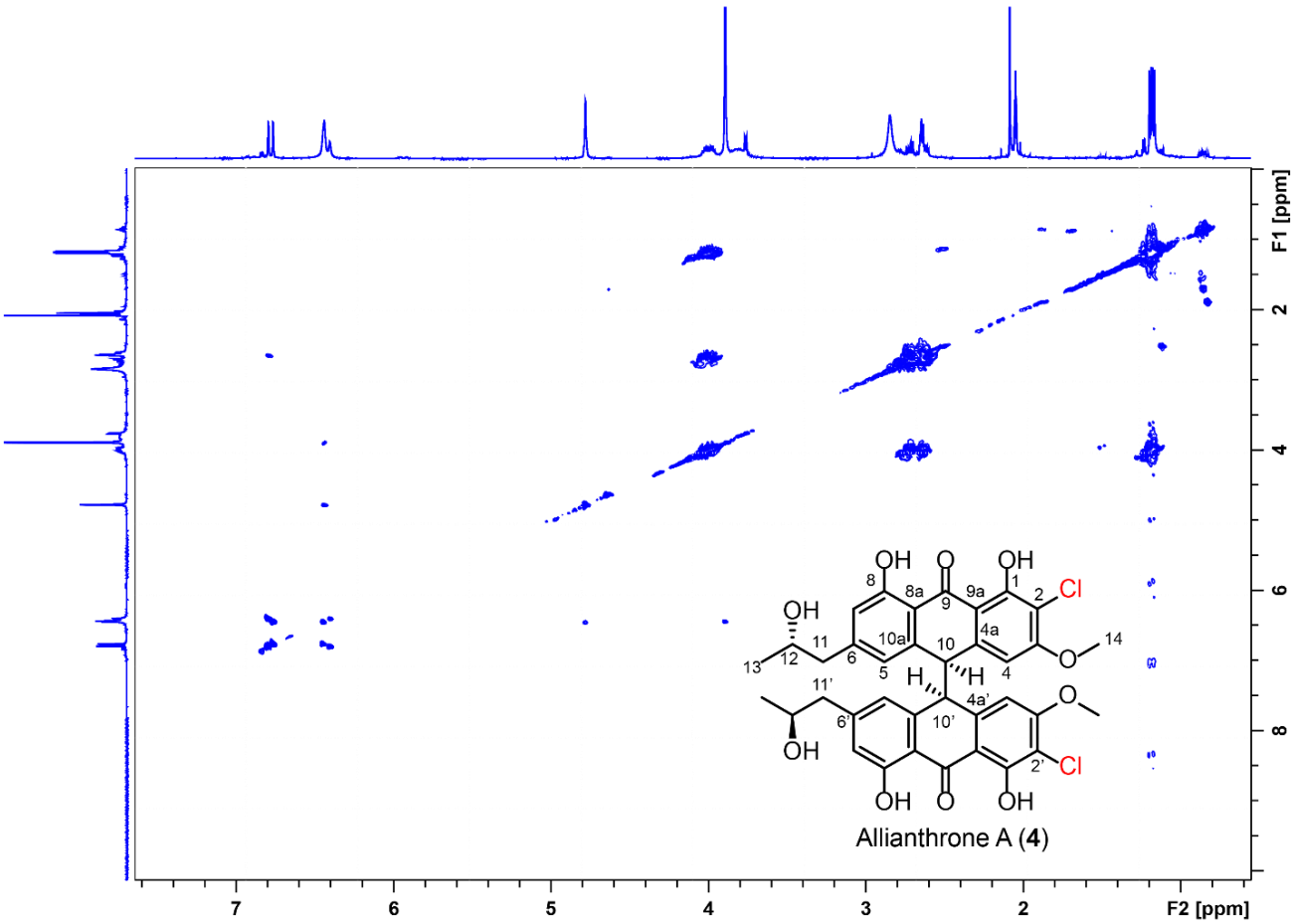

Figure S18: ^{1}H-^{1}H COSY NMR spectrum of compound **4** in acetone-d_3 at 500 MHz

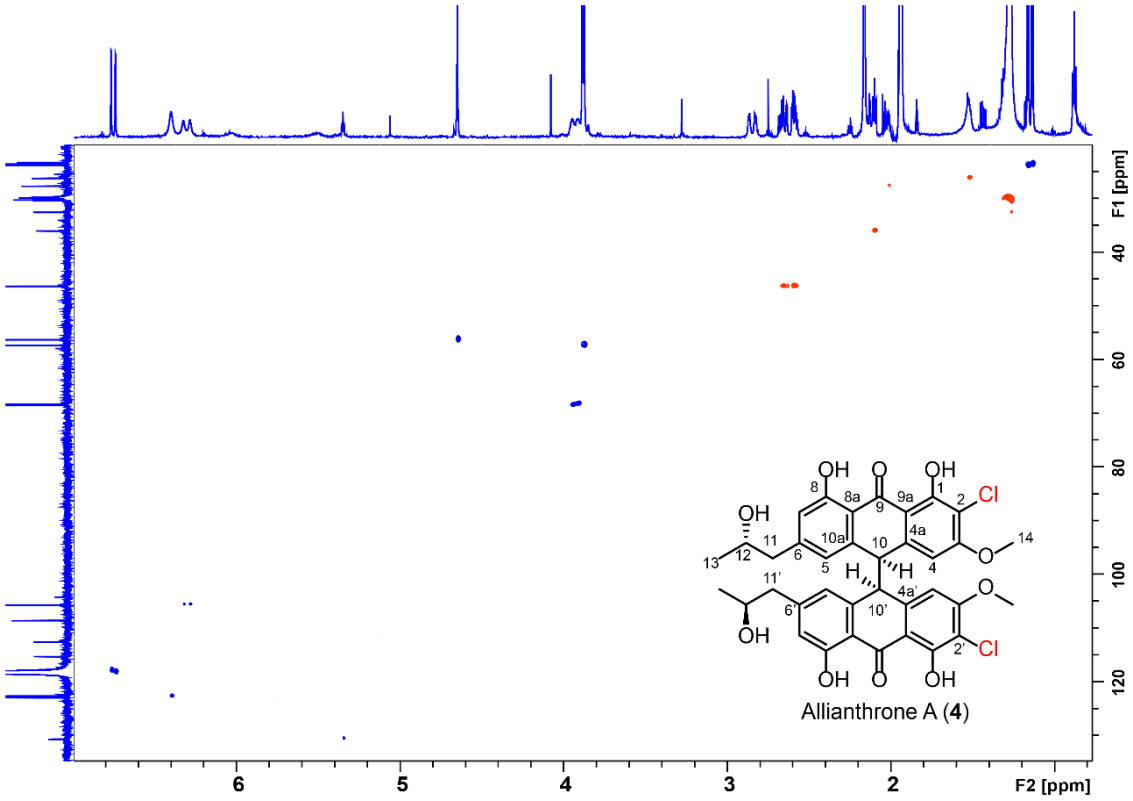

Figure S19: ^{1}H-^{13}C HSQC NMR spectrum of compound **4** in acetonitrile-d_3 at 700 MHz and 176 MHz

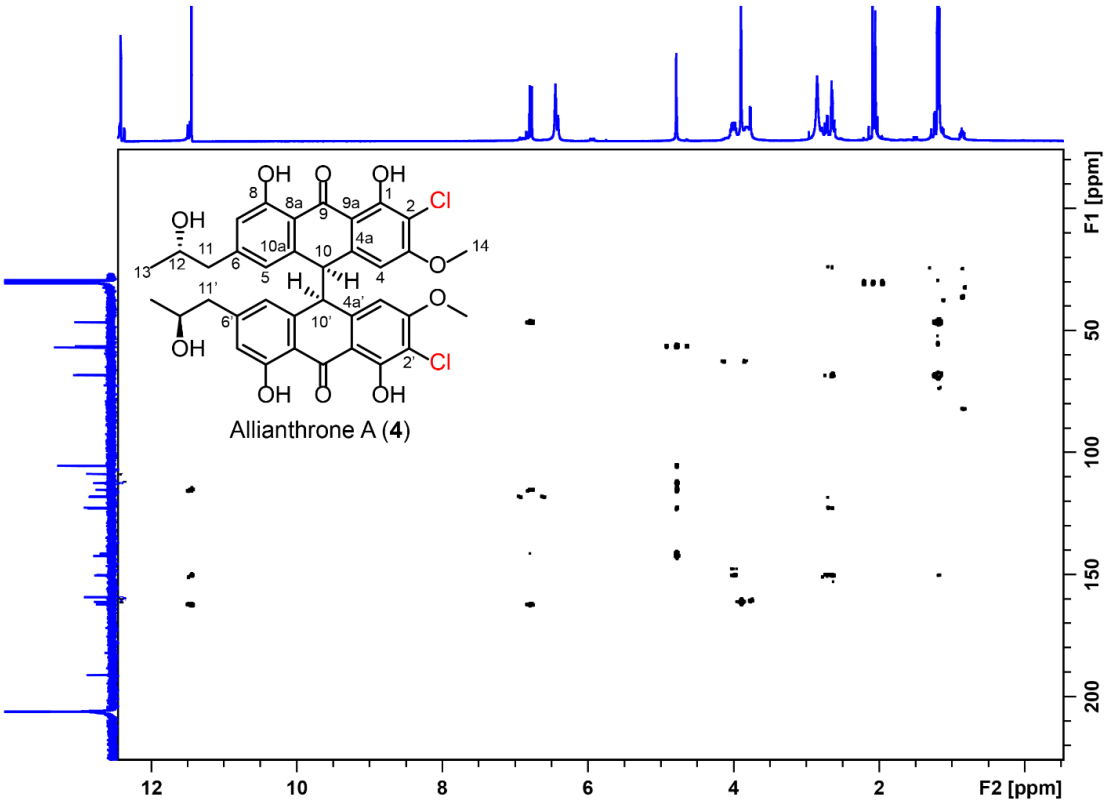

Figure S20: ^{1}H-^{13}C HMBC, 4 Hz optimized NMR spectrum of compound **4** in acetone-d_3 at 500 MHz and 125 MHz

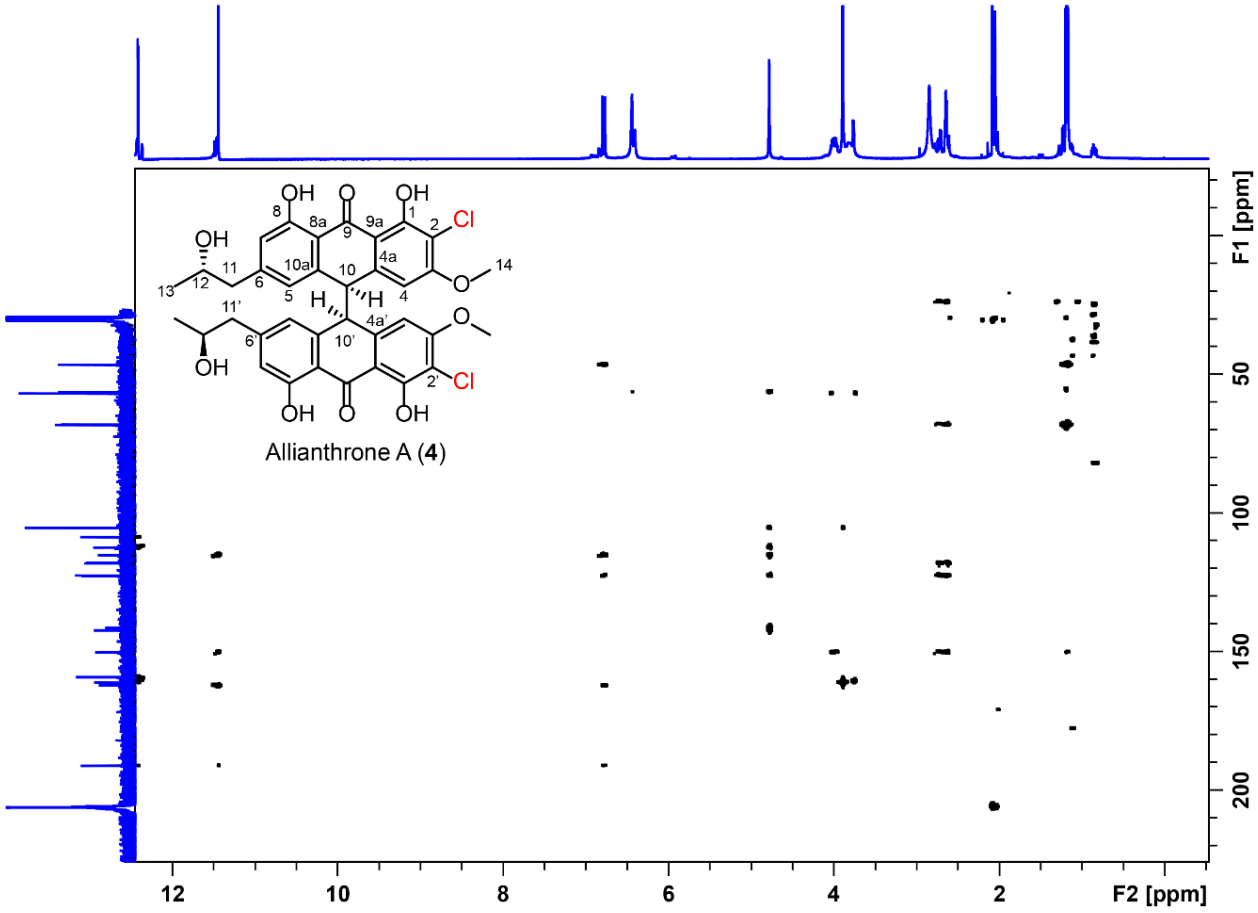

Figure S21: ^{1}H-^{13}C HMBC, 8 Hz optimized NMR spectrum of compound **4** in acetone-d_3 at 500 MHz and 125 MHz

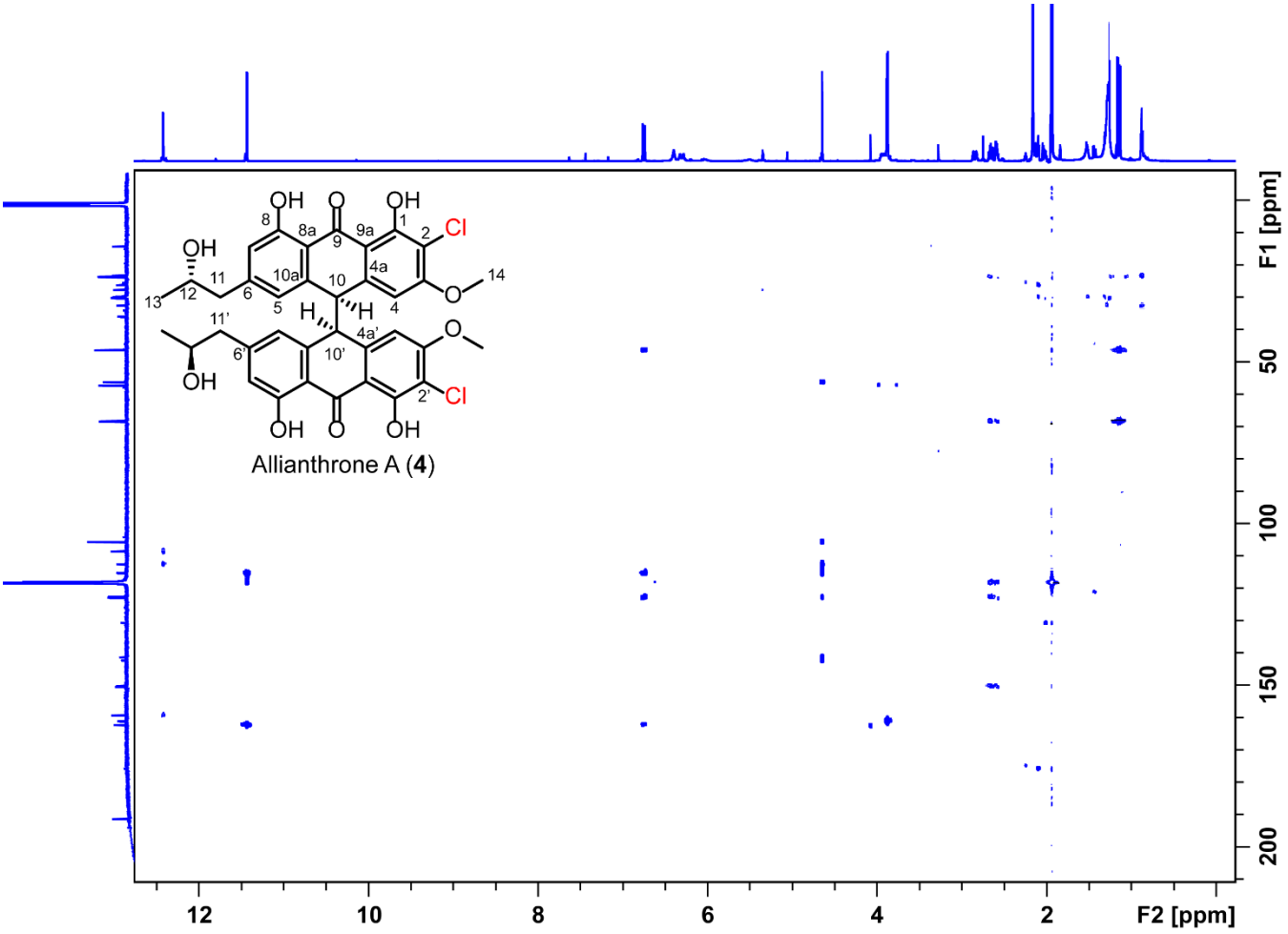

Figure S22: ^{1}H-^{13}C HMBC, 4 Hz optimized NMR spectrum of compound **4** in acetonitrile-d_3 at 700 MHz and 176 MHz

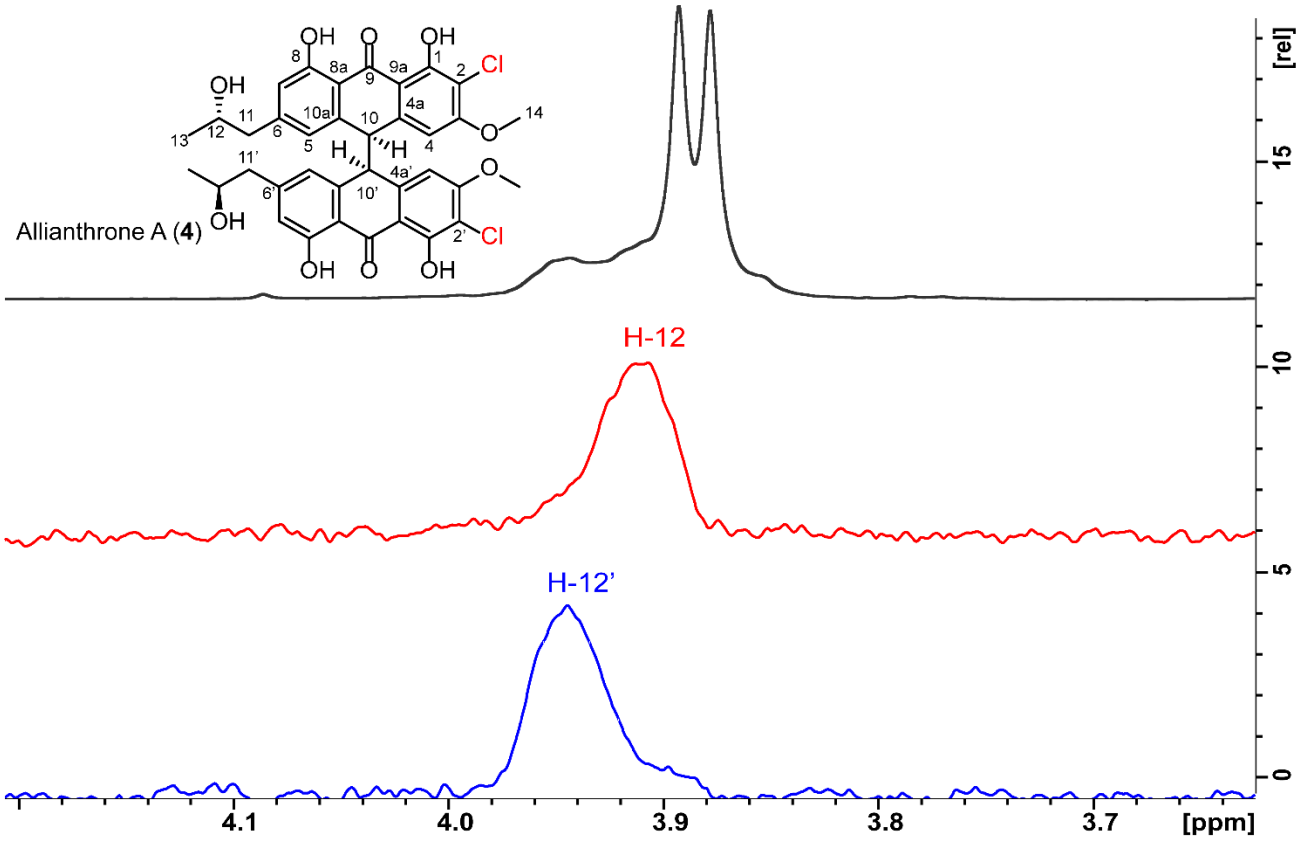

Figure S23: SEL-TOCSY of compound **4** in acetonitrile-d_3 at 700 MHz. Selective irradiation of H-13/13' established the identity of H-12 as belonging to alpha ring system (red) and H-12'as belonging to the beta ring system (blue)

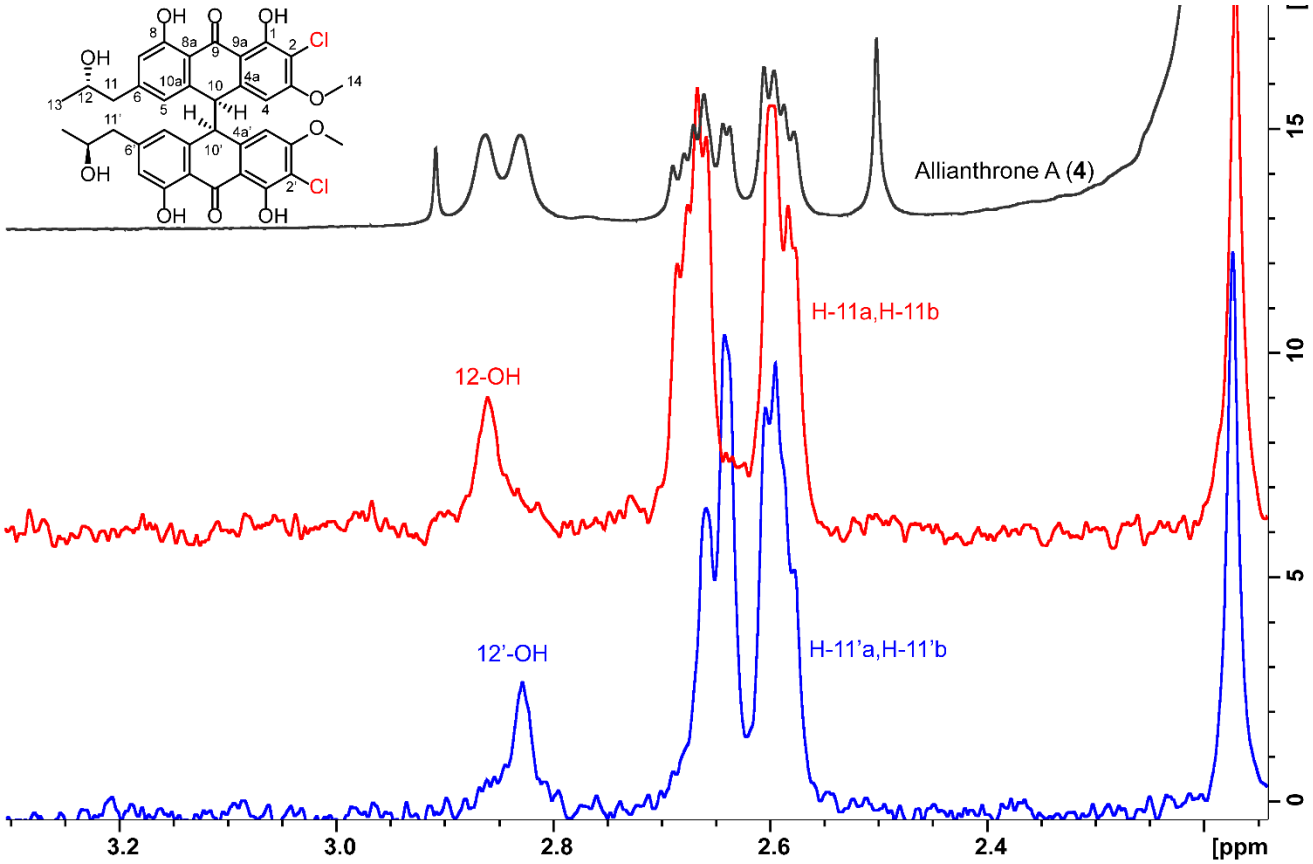

Figure S24: SEL-TOCSY of compound **4** in acetonitrile-d_3 at 700 MHz. Selective irradiation of H-13/13' established the identity of H-11a, H-11b and 12-OH as belonging to the alpha ring system (red) and H-11'a, H-11'b and 12'-OH as belonging to the beta ring system (blue)

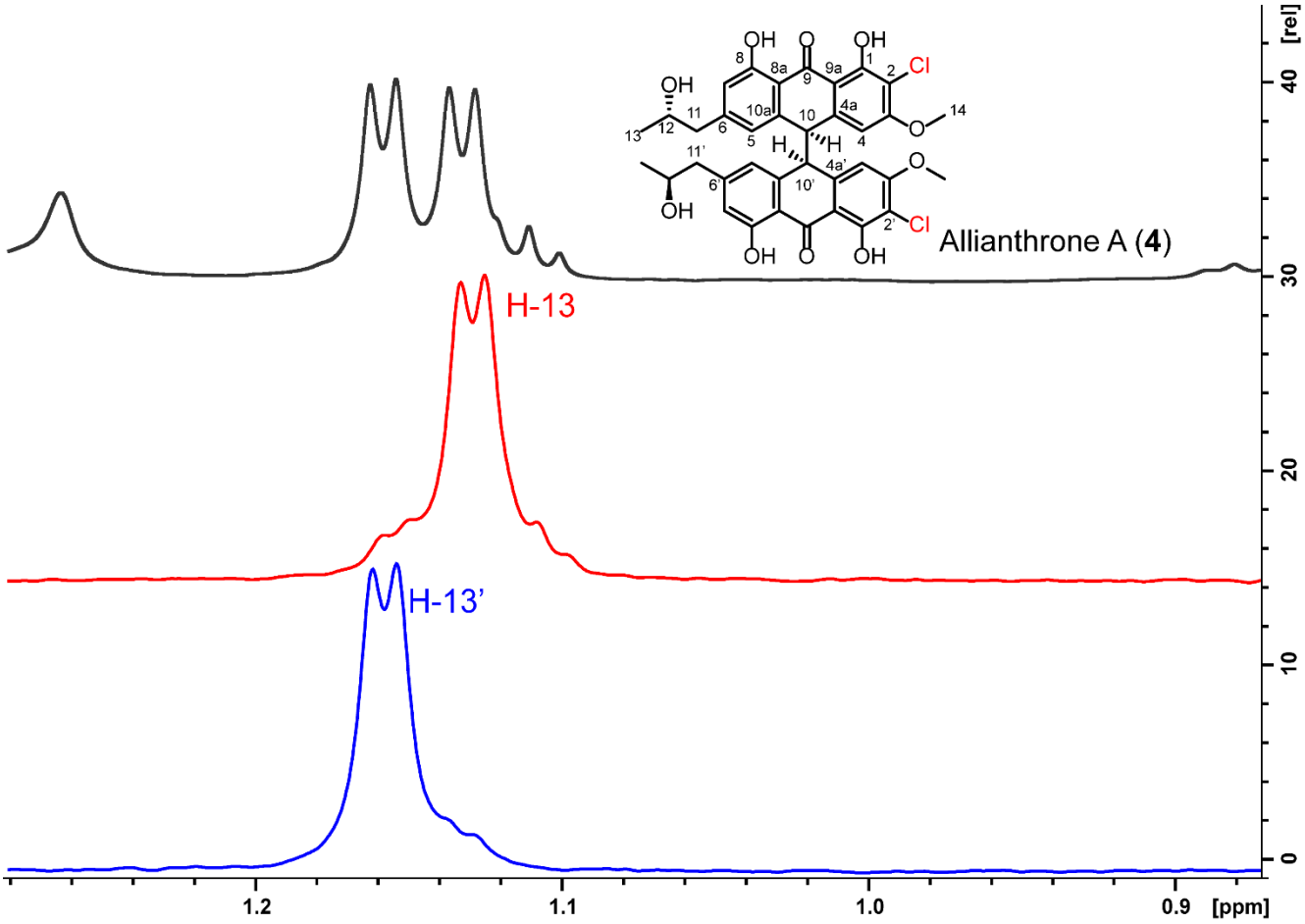

Figure S25: SEL-TOCSY of compound **4** in acetonitrile-d_3 at 700 MHz. Selective irradiation of H-13/13' established the identity of H-13 as belonging to the alpha ring system (red) and H-13'as belonging to the beta ring system (blue)

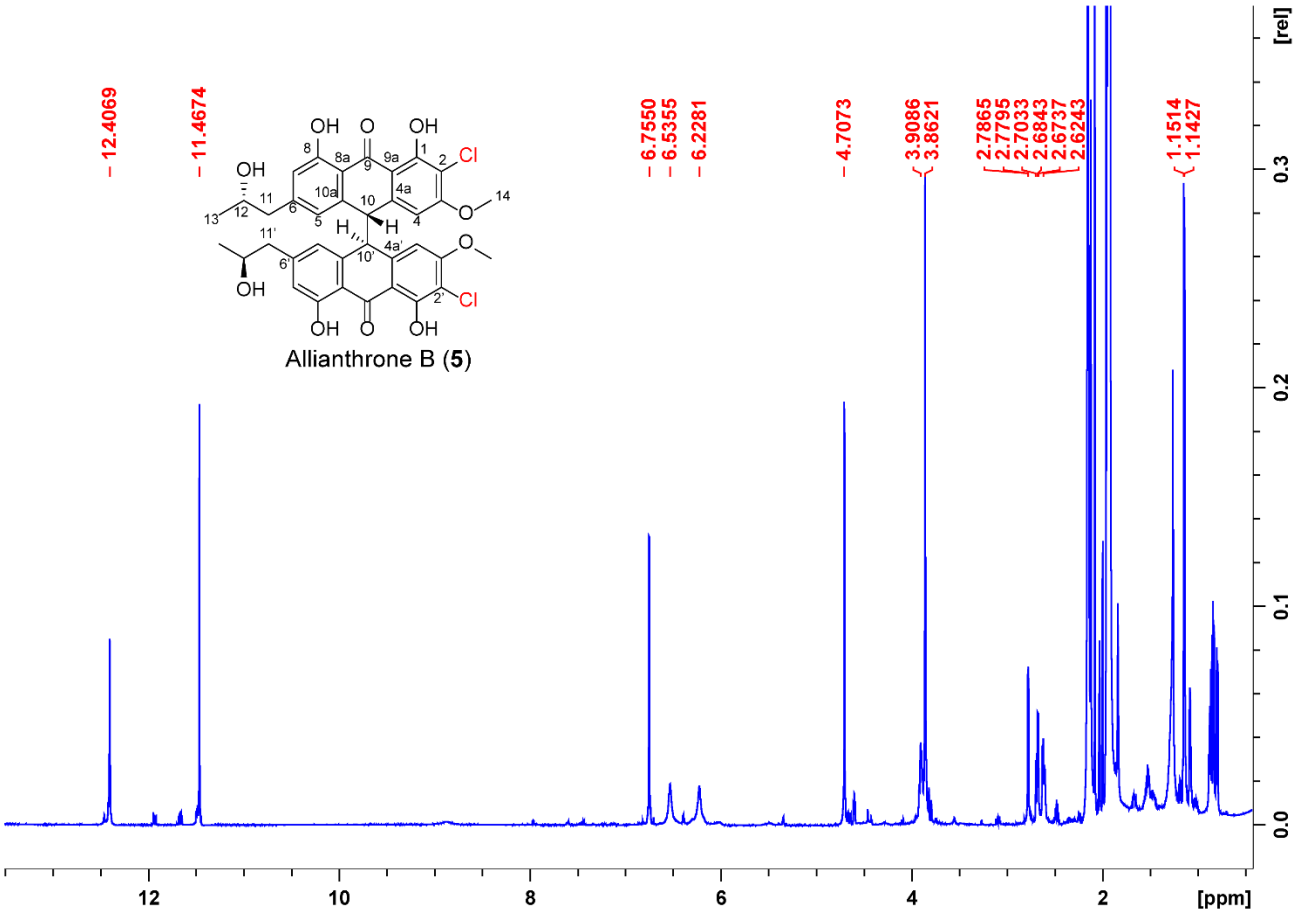

Figure S26: ^{1}H NMR spectrum of compound **5** in acetonitrile-d_3 at 700 MHz

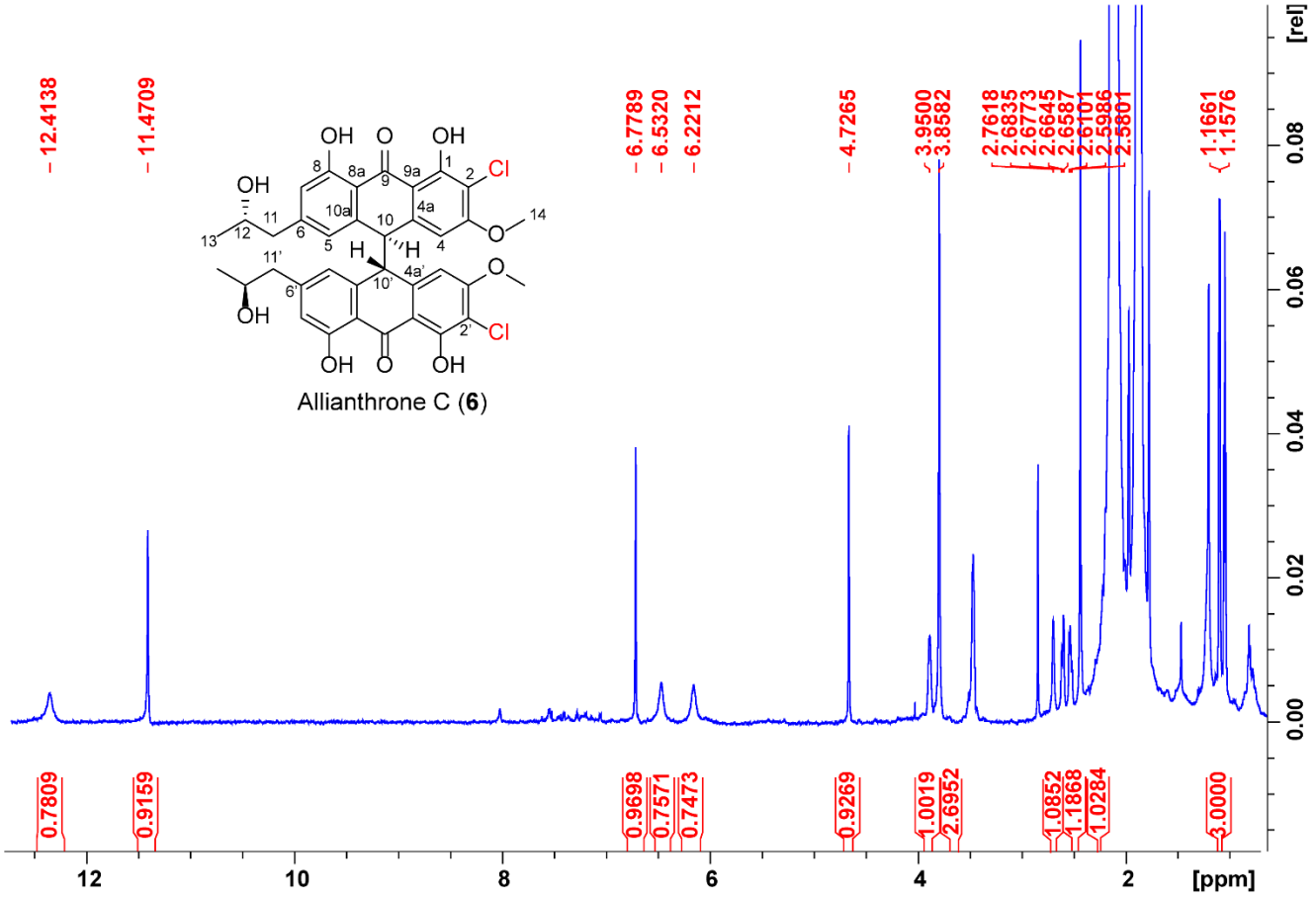

Figure S27: ^{1}H NMR spectrum of compound **6** in acetonitrile-d_3 at 700 MHz

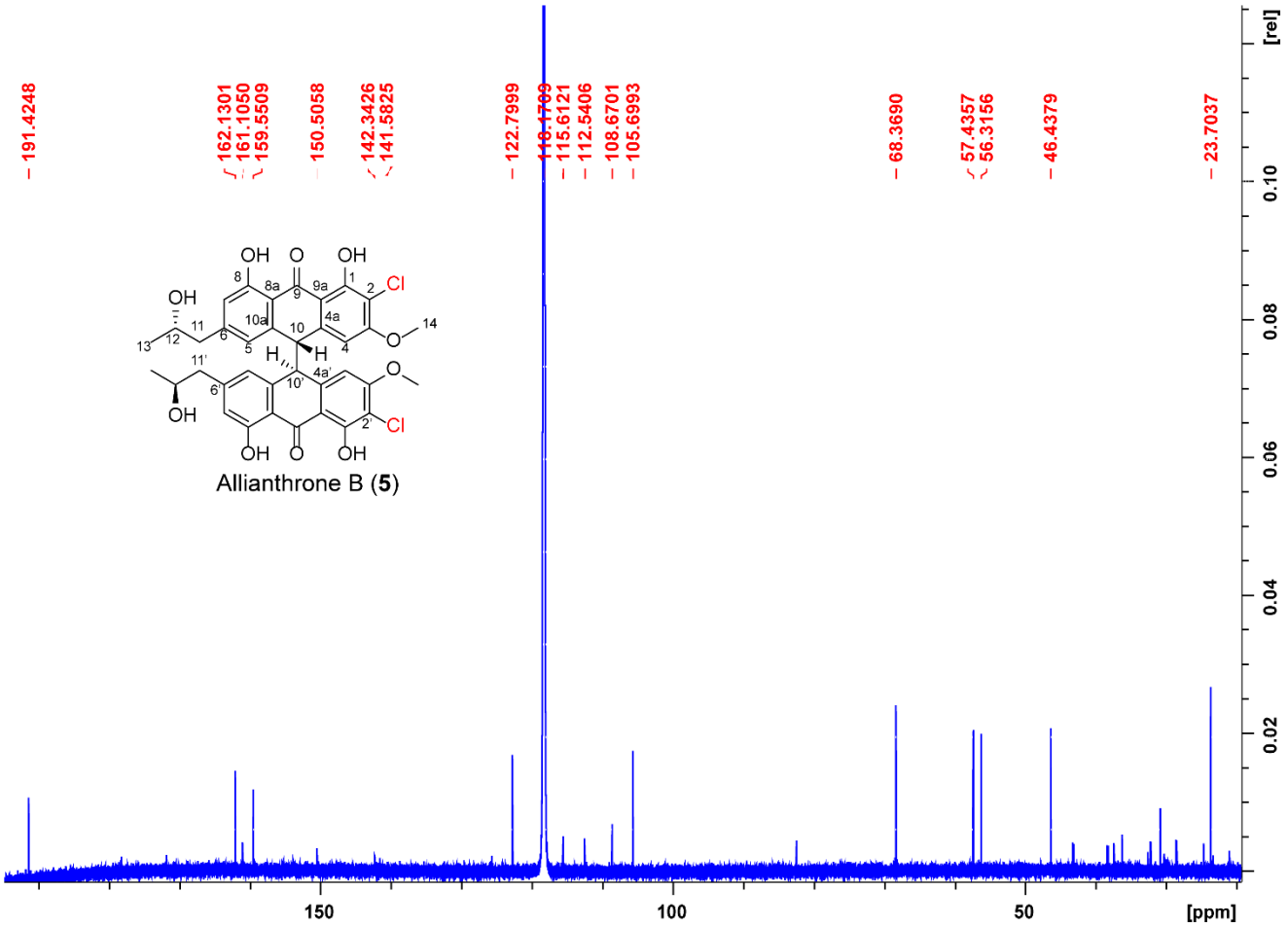

Figure S28: ^{13}C NMR spectrum of compound **5** in acetonitrile-d_3 at 176 MHz

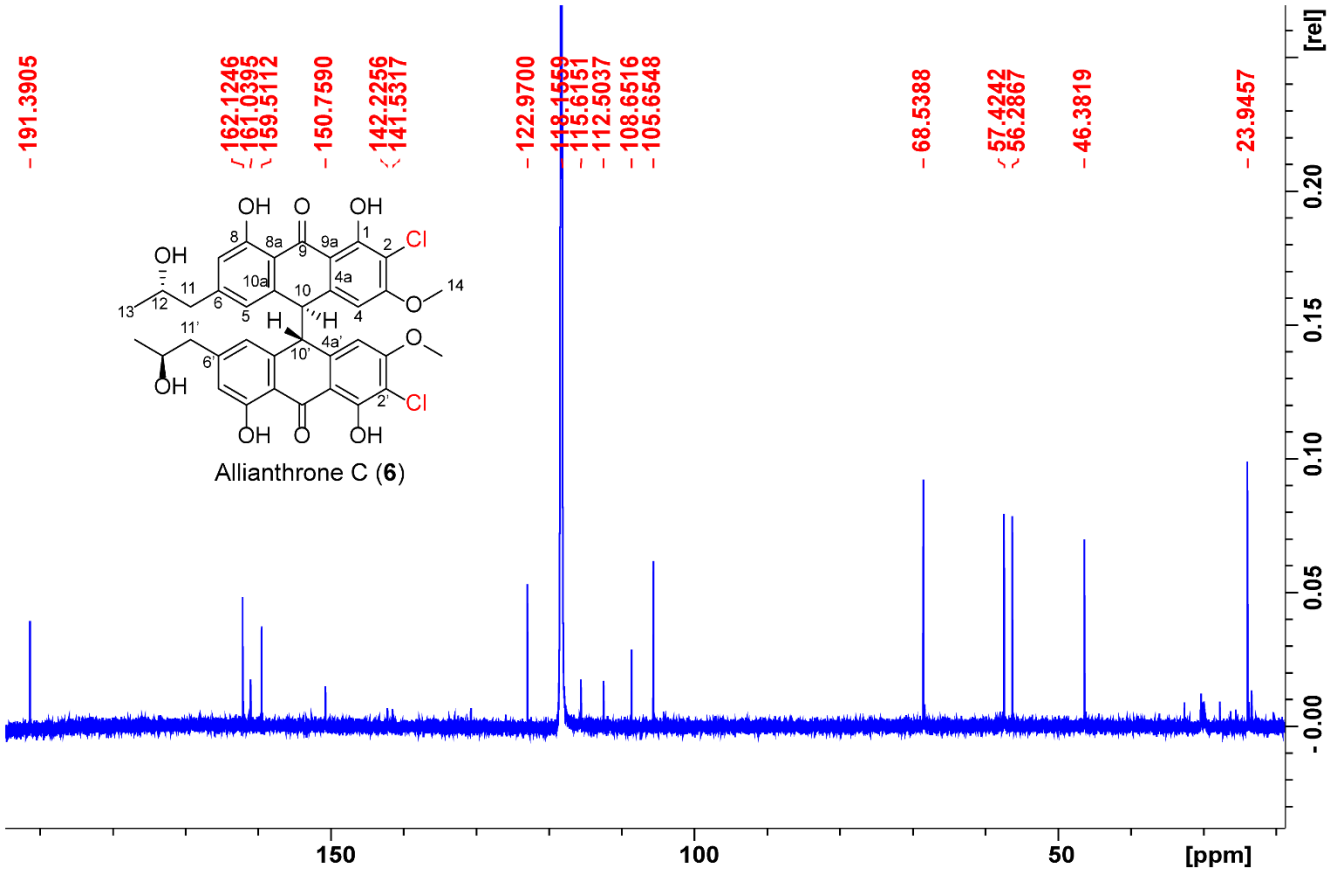

Figure S29: ^{13}C NMR spectrum of compound **6** in acetonitrile-d_3 at 176 MHz

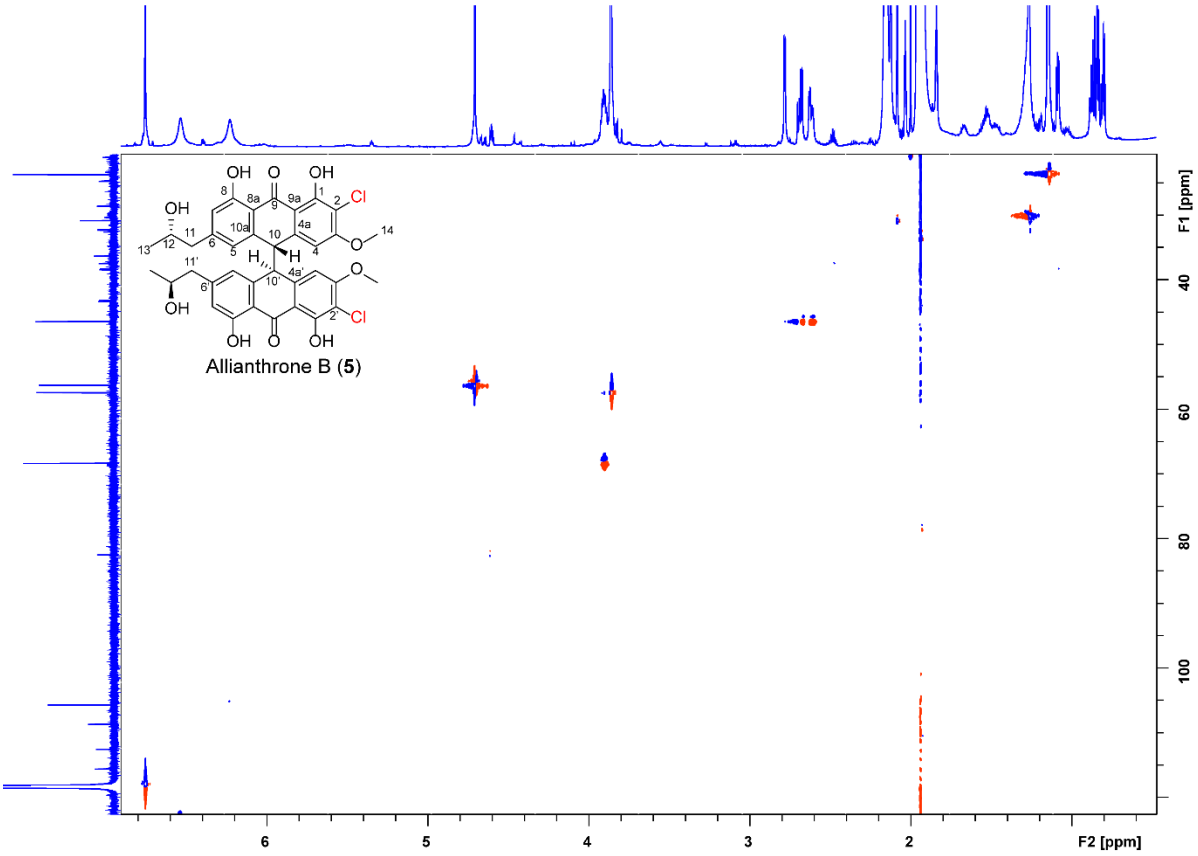

Figure S30: ^{1}H-^{13}C HSQC NMR spectrum of compound **5** in acetonitrile-d_3 at 700 MHz and 176 MHz

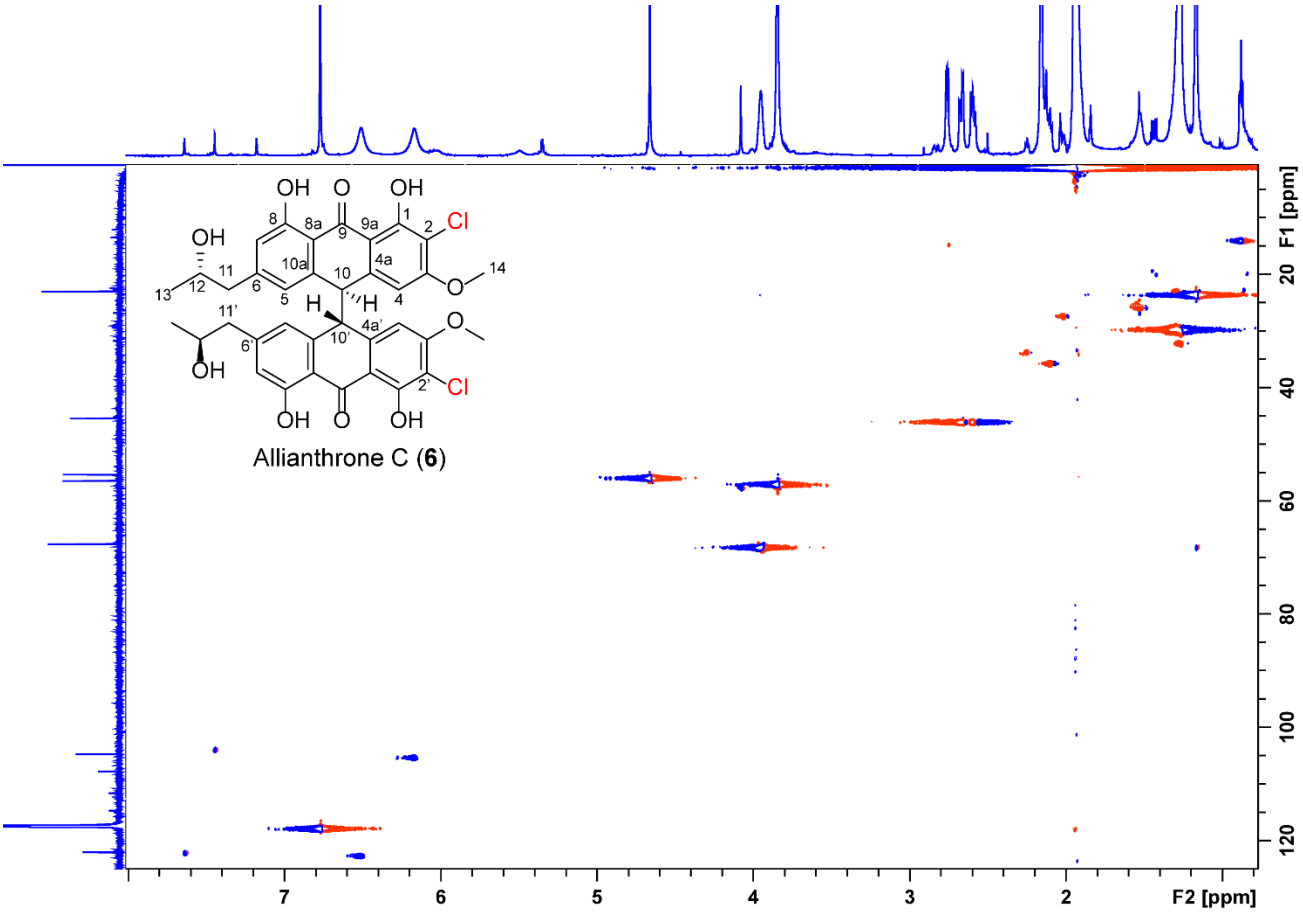

Figure S31: ^{1}H-^{13}C HSQC NMR spectrum of compound **6** in acetonitrile-d_3 at 700 MHz and 176 MHz

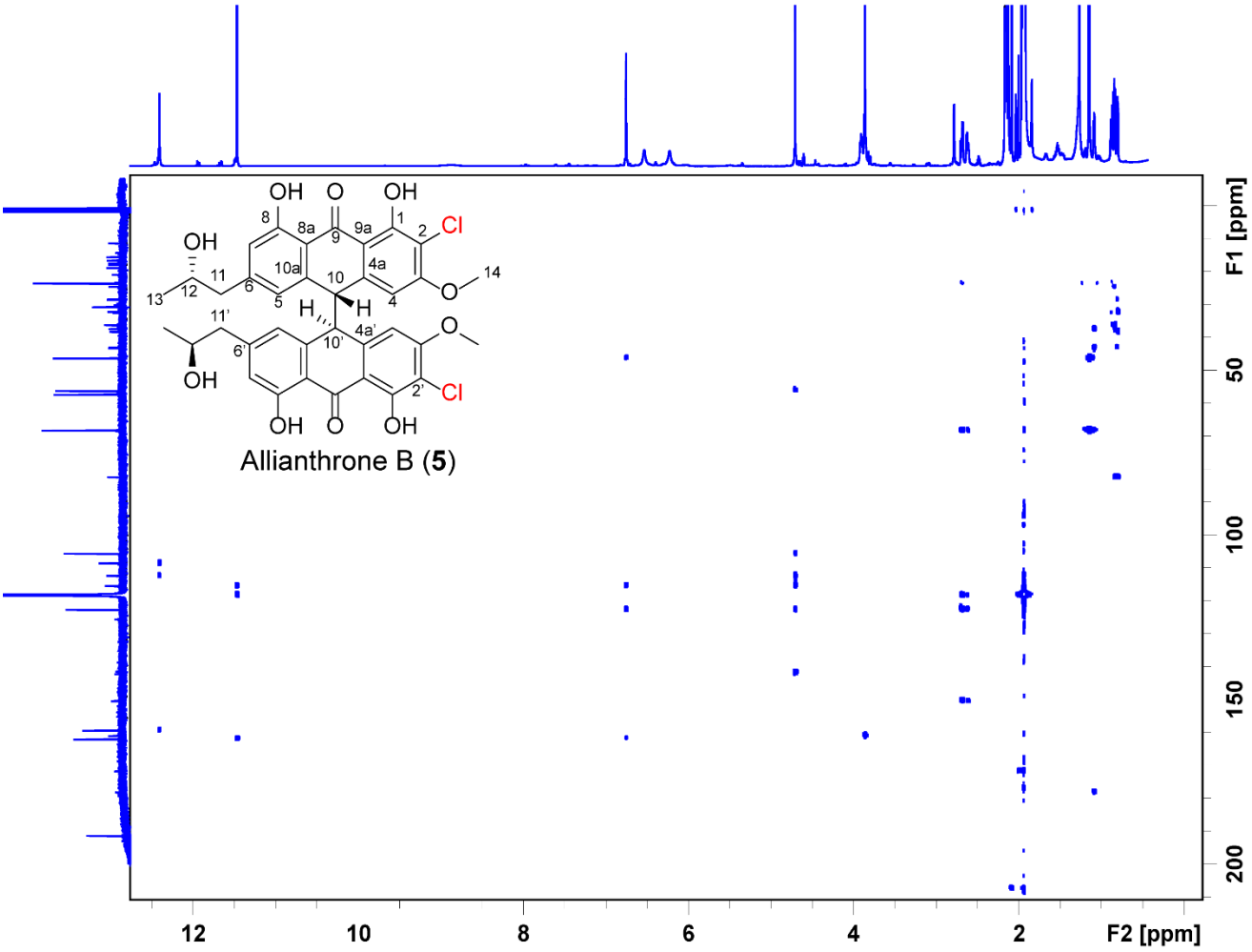

Figure S32: ^{1}H-^{13}C HMBC, 4 Hz optimized NMR spectrum of compound **5** in acetonitrile-d_3 at 700 MHz and 176 MHz

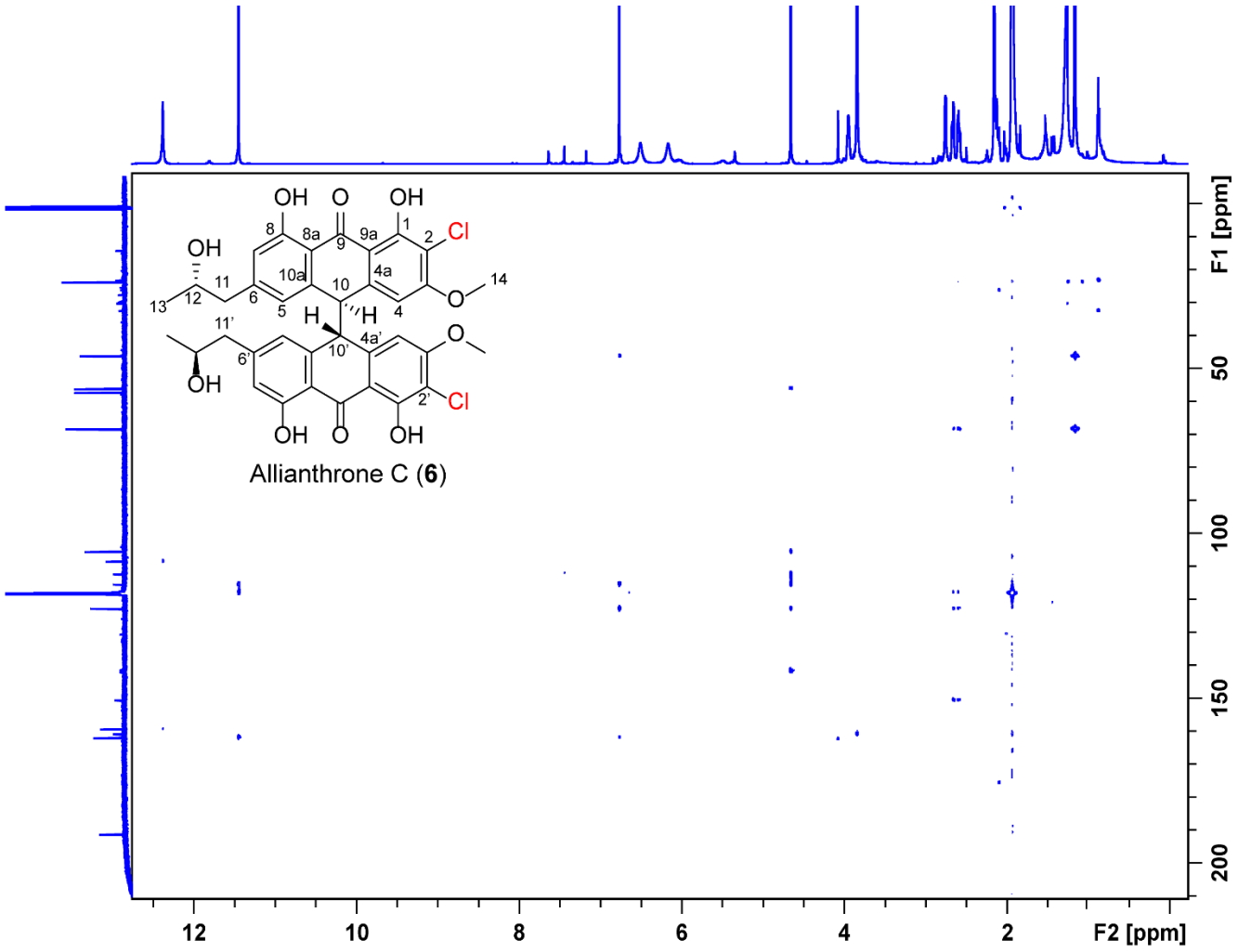

Figure S33: ^{1}H-^{13}C HMBC, 4 Hz optimized NMR spectrum of compound **6** in acetonitrile-d_3 at 700 MHz and 176 MHz

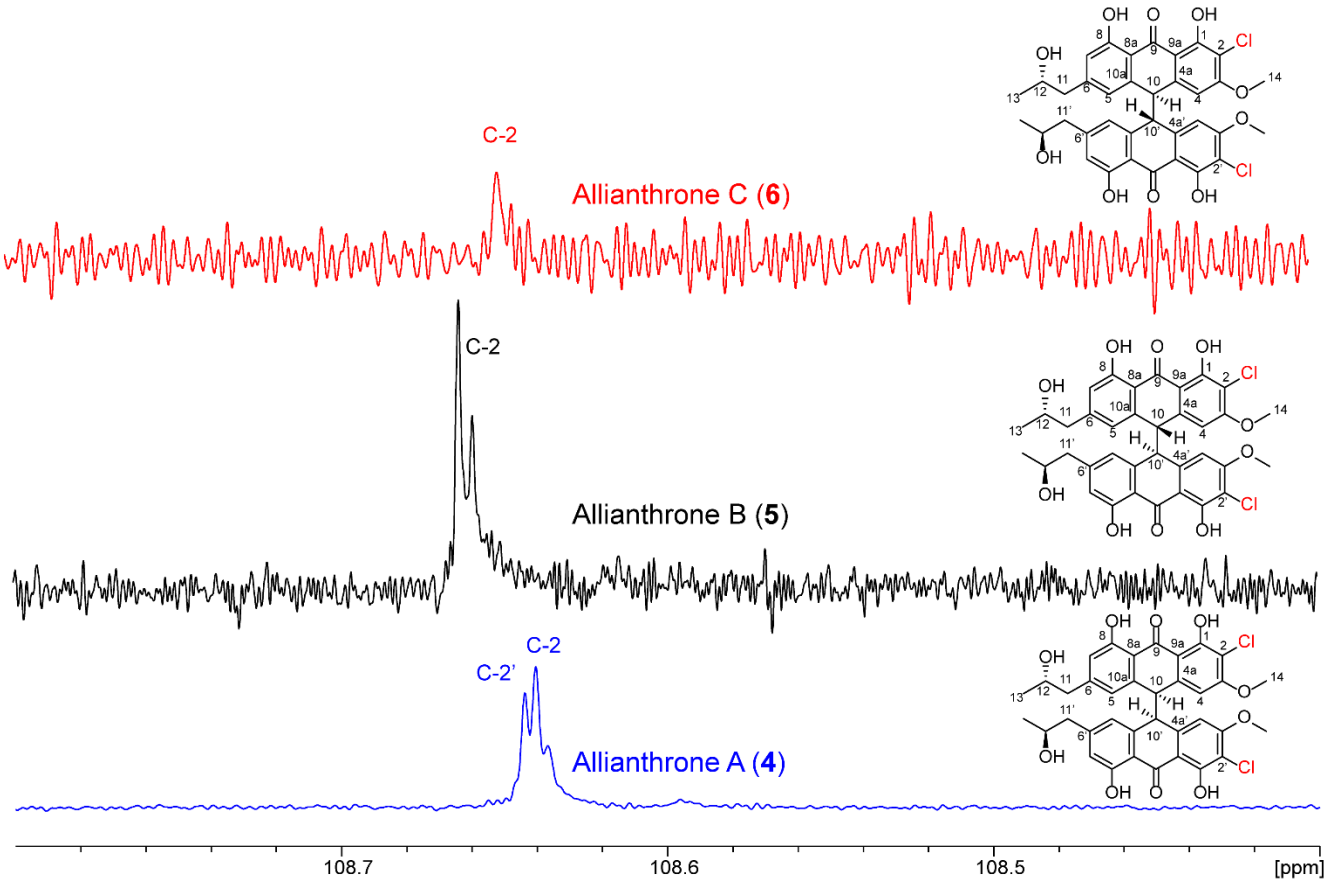

Figure S34: Ultra-high resolution ^{13}C NMR of compounds **4**, **5**, and **6** in acetonitrile-d_3 with $^{37}Cl/^{35}Cl$ isotope shifts evident in the C-2 carbon signal. **4** exhibits non-chemical equivalence between the anthronyl rings, and thus exhibits two chlorine isotope effects for C-2 and C-2', while **5** and **6** are have chemically equivalent anthronyl rings and exhibit a single C-2 singlet with a Cl isotope shift.

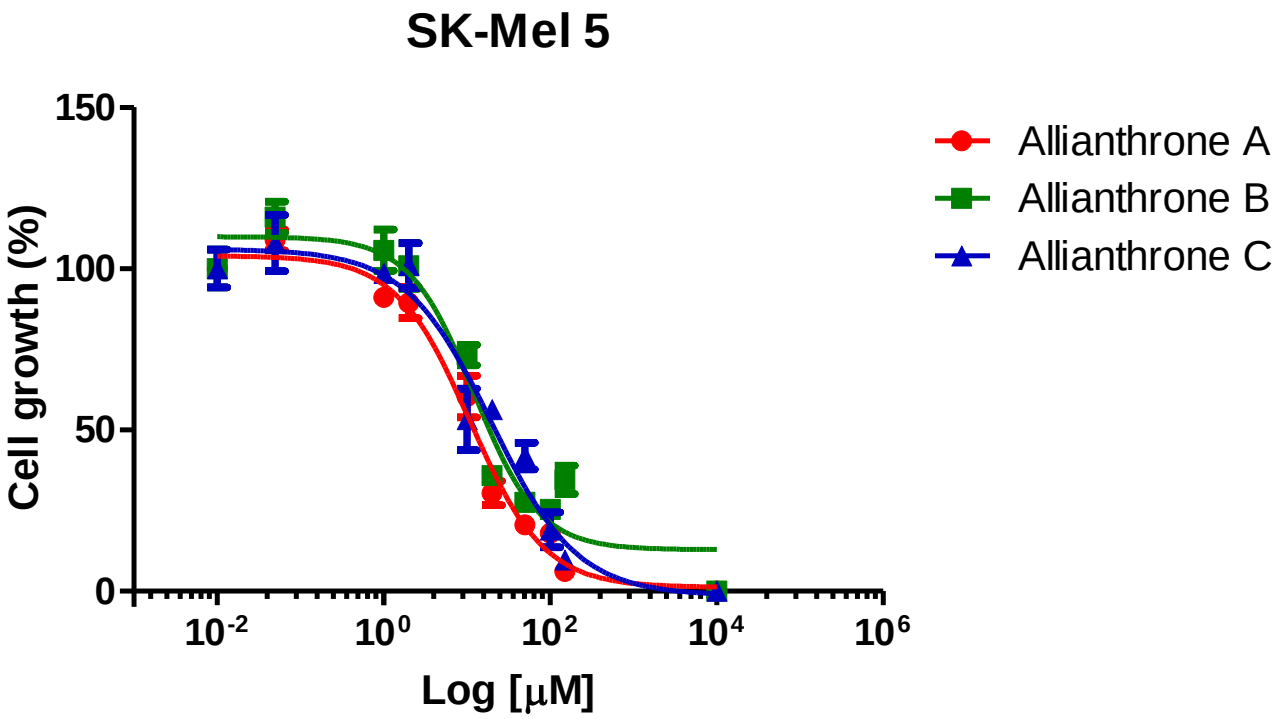

Figure S35: IC50 curve of compounds **4-6** against SK-Mel 5

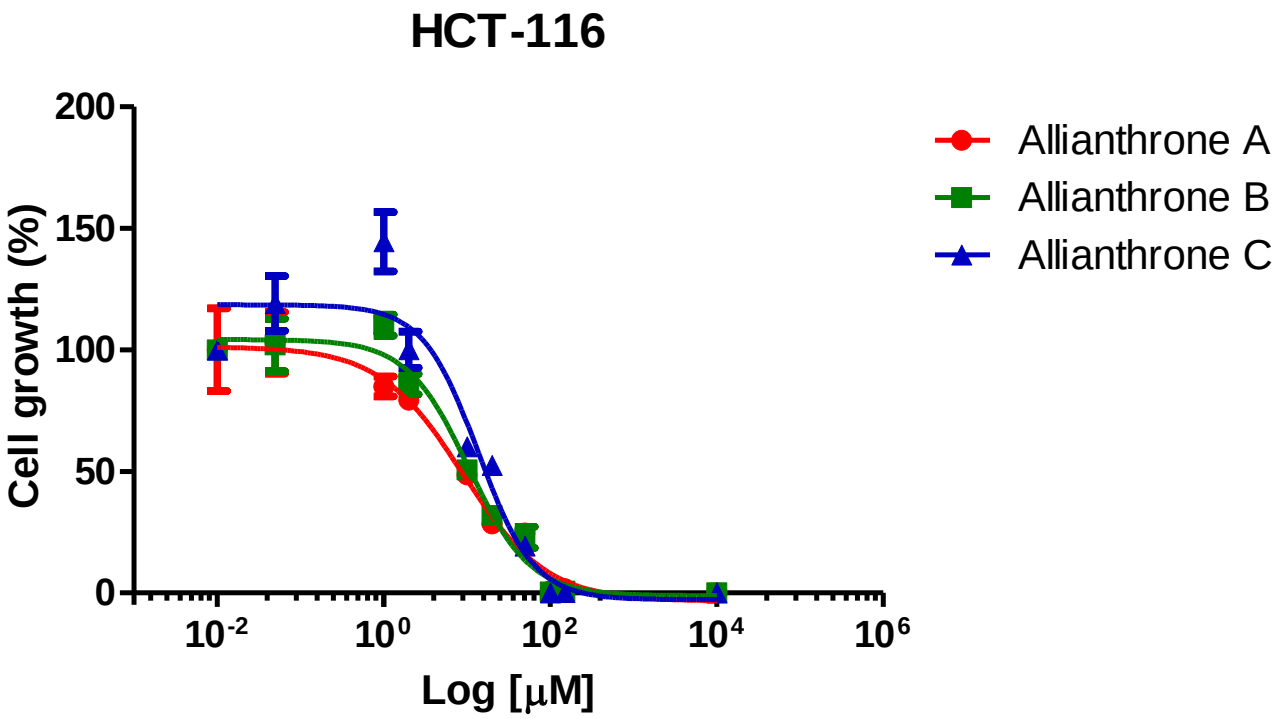

Figure S36: IC50 curve of compounds **4-6** against HCT-116

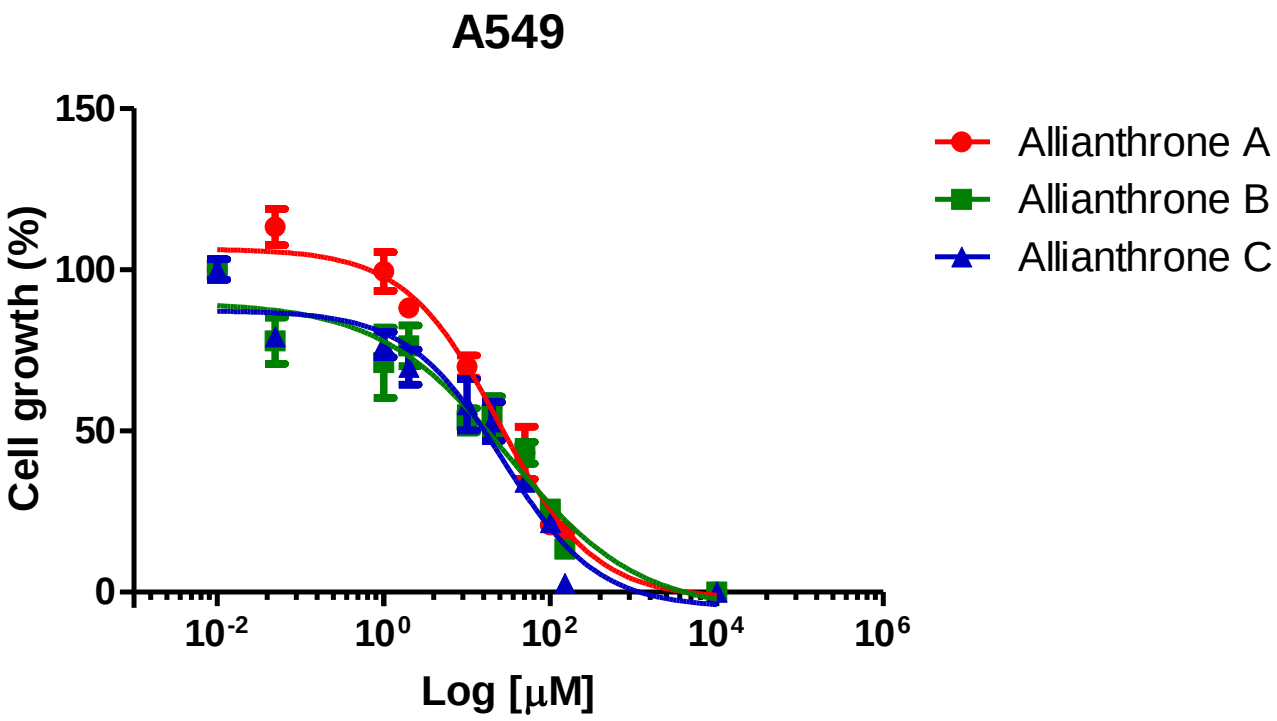

Figure S37: IC50 curve of compounds **4-6** against A549

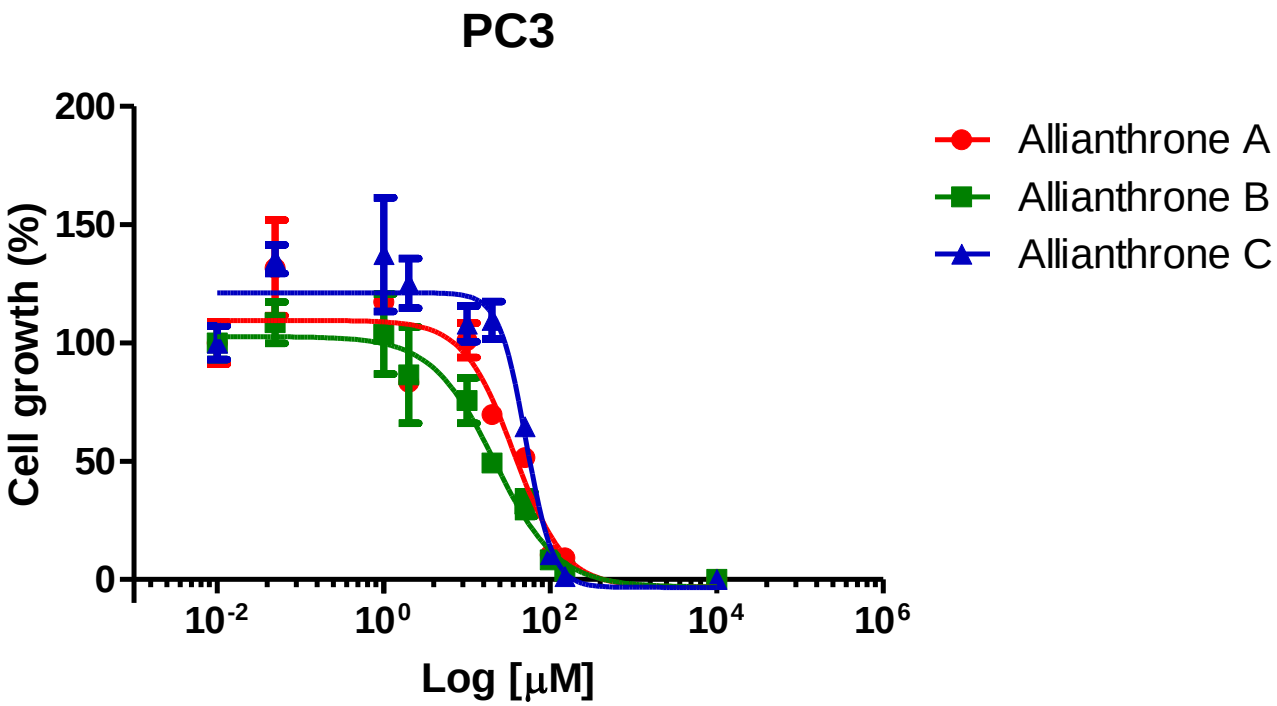

Figure S38: IC50 curve of compounds **4-6** against PC3

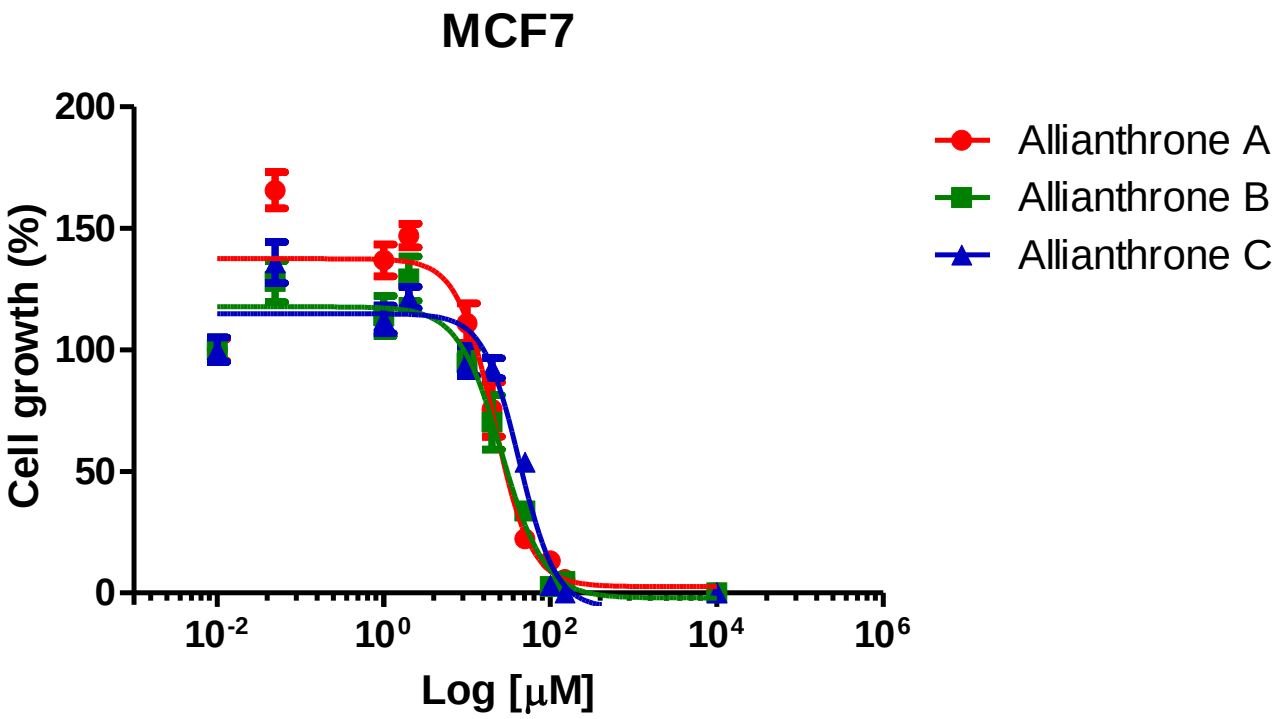

Figure S39: IC50 curve of compounds **4-6** against MCF7

Figure S40: Antimcirobial single-dose microbroth assay with nalgiovensin (20.5 µg/mL), nalgiolaxin (22.7 µg/mL), and allianthrones A-C (43.5 µg/mL). Control antibiotic (125 µg/mL) used: chloramphenicol (*Bacillus subtilis* ATCC 49343), ampicillin (*Escherichia coli* ATCC 8739), kanamycin (*Pseudomonas aeruginosa* (ATCC 15442), *Staphylococcus aureus* ATCC 25923), vancomycin (*Enterococcus faecium* ATCC 49032), and amphotericin B (*Candida albicans* ATCC 90027). Ethanol was used as the negative control at 1.25 %v/v.

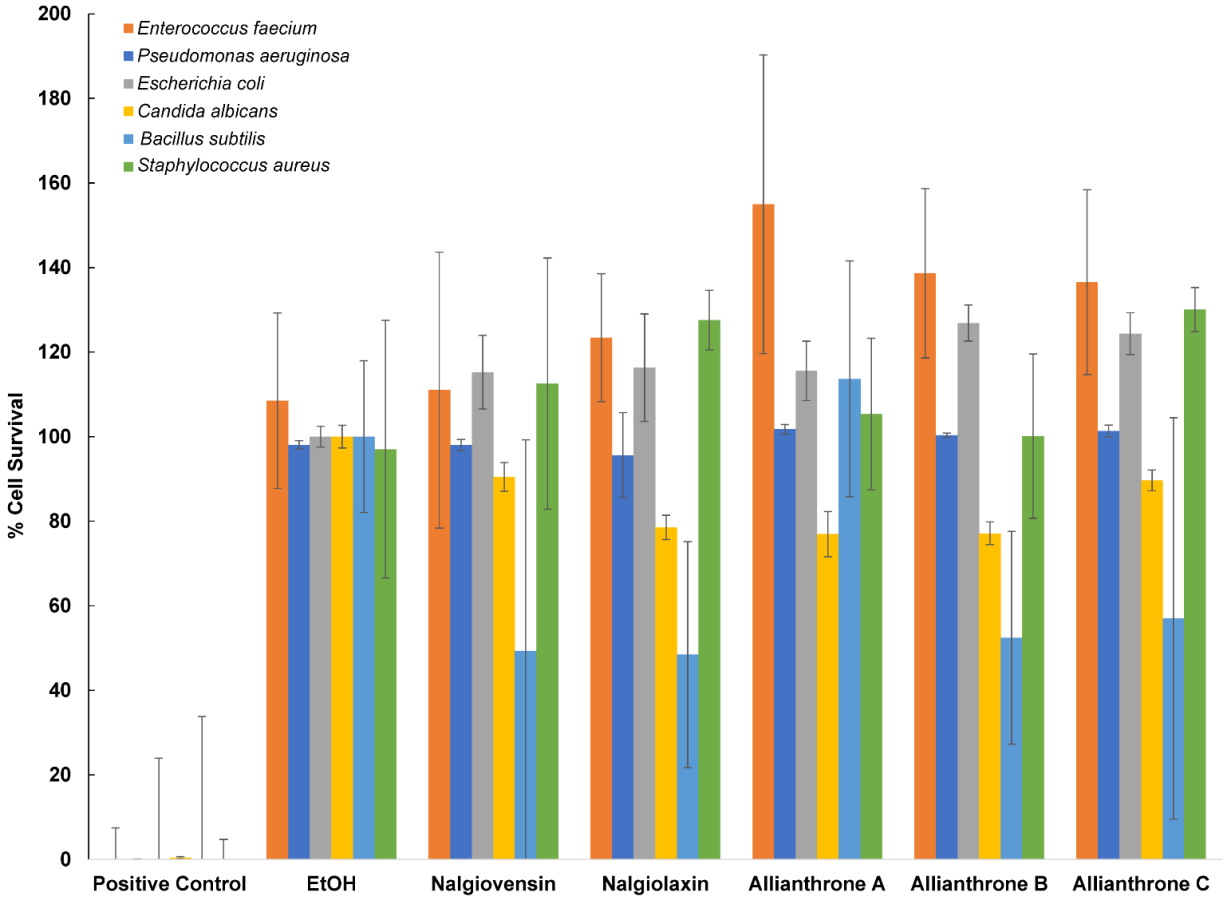

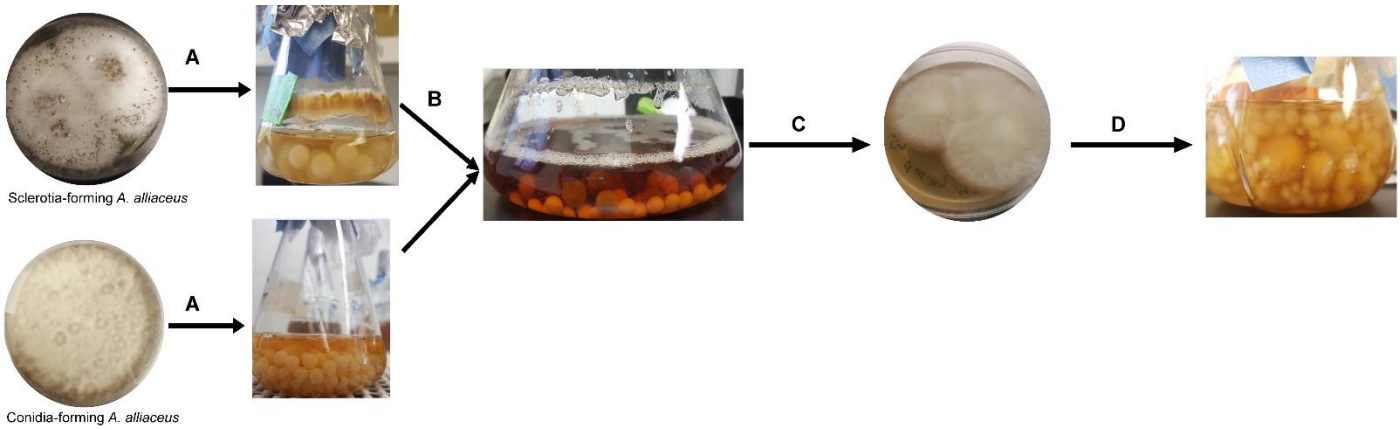

Figure S41: A) Sclerotia-forming and conidia-forming phenotype of *A. alliaceus* on agar plates were propagated into malt-based broth media and grown for 14 days in separate flasks. B) After 14 days of growth, the mycelia from each flask were combined into a single flask containing buffered-malt broth and placed on a 200 rpm shaker at ambient light and temperature for 15-20 days. C) Before extraction, the flask of combined mycelia was streaked out and a phenotypic change was observed, different compared to either starting phenotypes. D) The metabolically activated *A. alliaceus* was propagated into another flask containing buffered-malt broth and grown for 15-20 days.

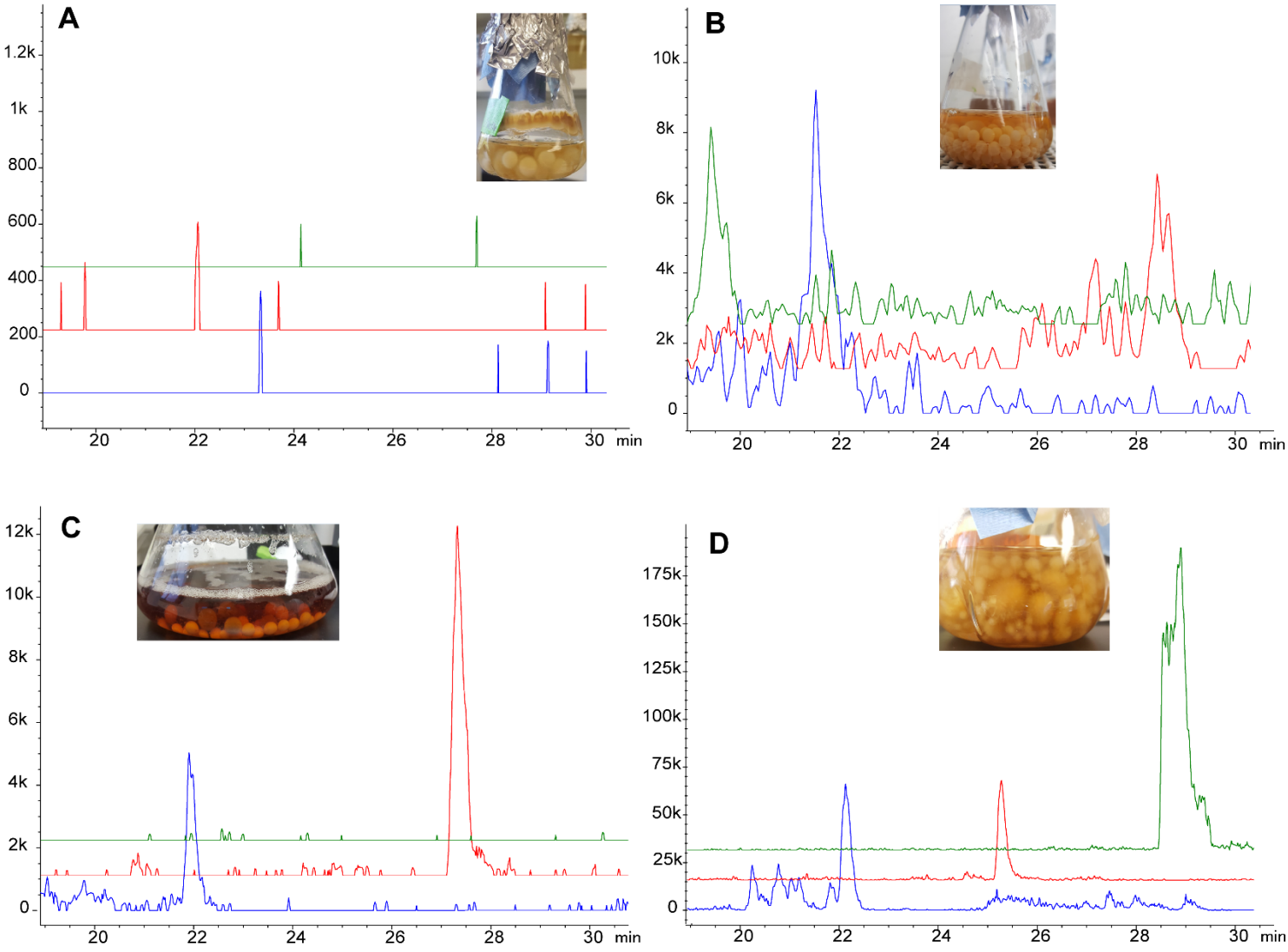

Figure S42: Extracted ion chromatographs at day 15 of culture to detect compounds **2** (blue), **3** (red), and **4-6** (green) in A) sclerotia-forming *A. alliaceus*, B) conidia-forming *A. alliaceus*, C) combined hyphae of sclerotia-forming and conidia-forming *A. alliaceus*, and D) coculture induced phenotype. Bianthrone formation is only observed after coculture activation

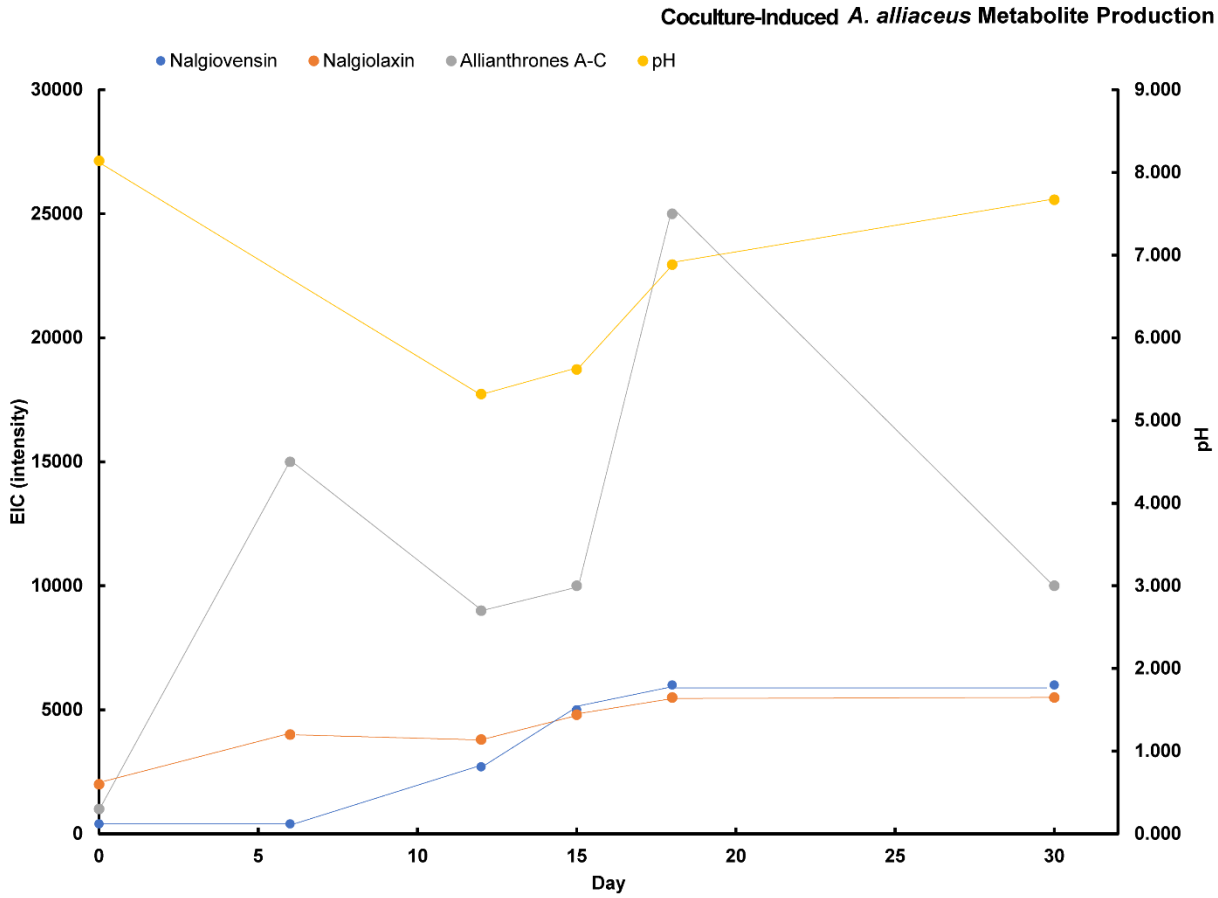

Figure S43: Production of **2-6** from phenotype coculture induced *Aspergillus alliaceus* monitored by extracted ion chromatography LCMS. Bianthrone production (gray) peaks around day 20, pH of the culture is also presented in yellow.

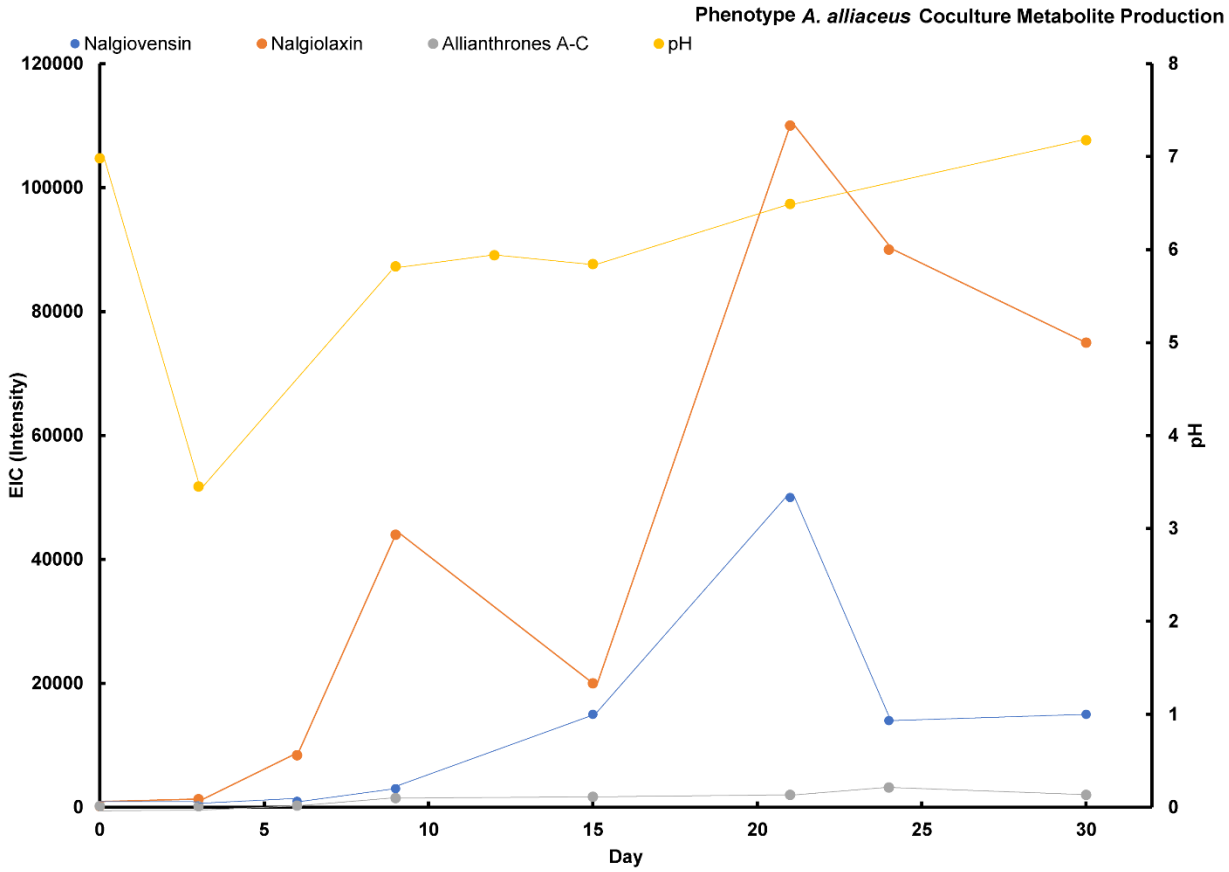

Figure S44: Production of **2-6** in a fresh initiated mixed culture of sclerotia-forming and conidia-forming *Aspergillus alliaceus* monitored by extracted ion chromatography LCMS. Bianthrone production (gray) is not observed in freshly combined fungal cultures. pH of the culture is presented in yellow.

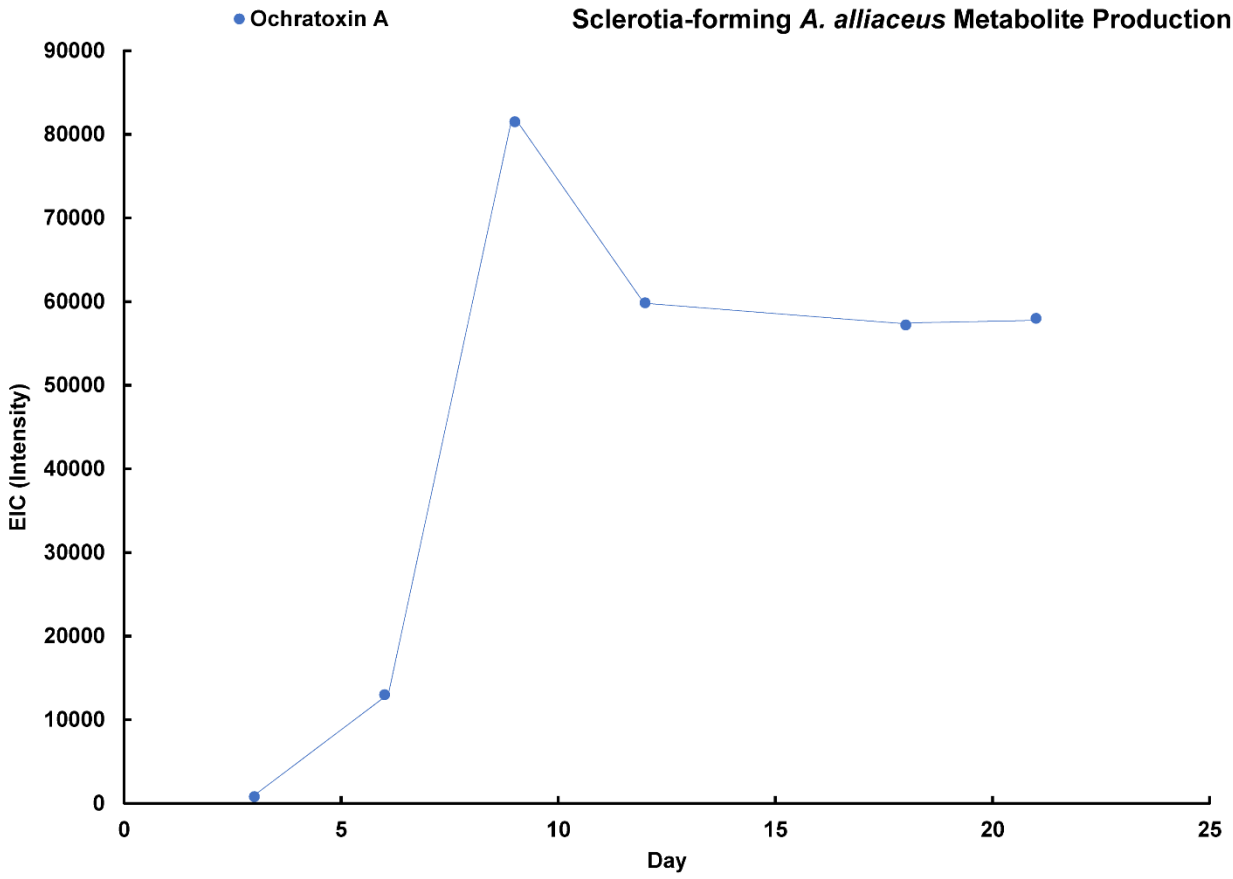

Figure S45: Production of **1** by sclerotia-forming *Aspergillus alliaceus* monitored by extracted ion chromatography LCMS.

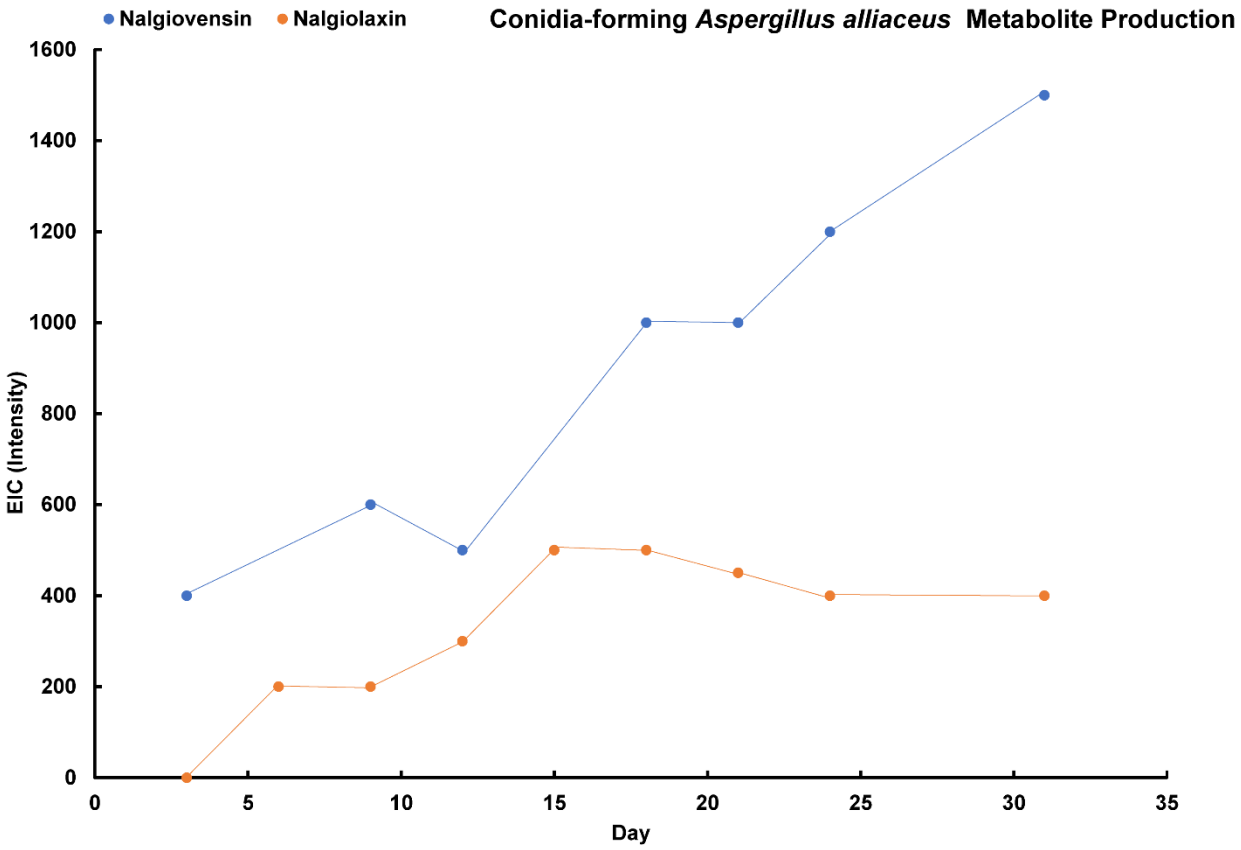

Figure S46: Production of **2** and **3** by conidia-forming *Aspergillus alliaceus* monitored by extracted ion chromatography LCMS.

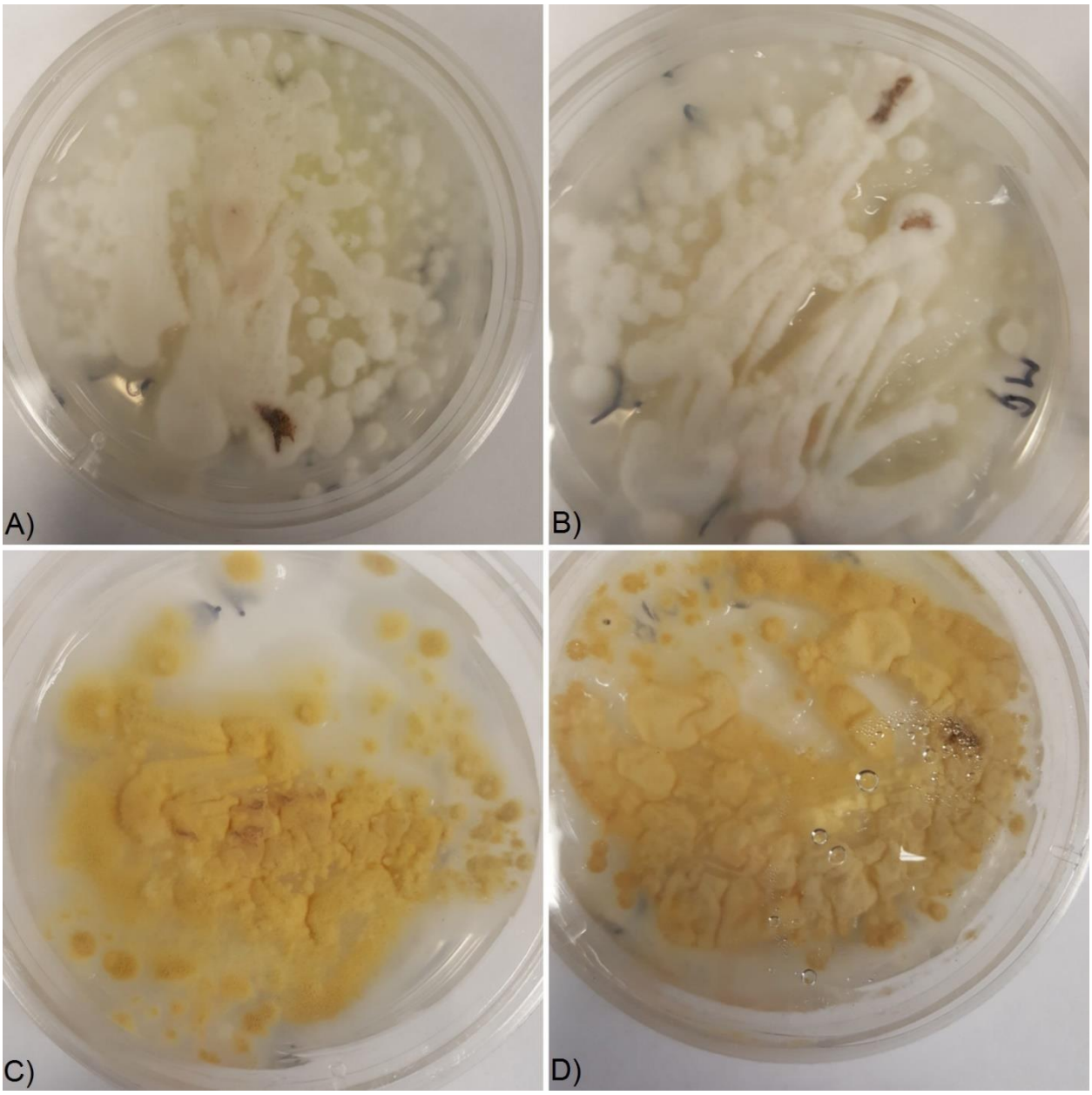

Figure S47: Conidia-forming *A. alliaceus* phenotype study on Czapek-Dox agar under A) no light, 25°C, B) light, 25°C, C) no light, 37°C and D) light, 37°C with photos taken between five and seven days of growth.

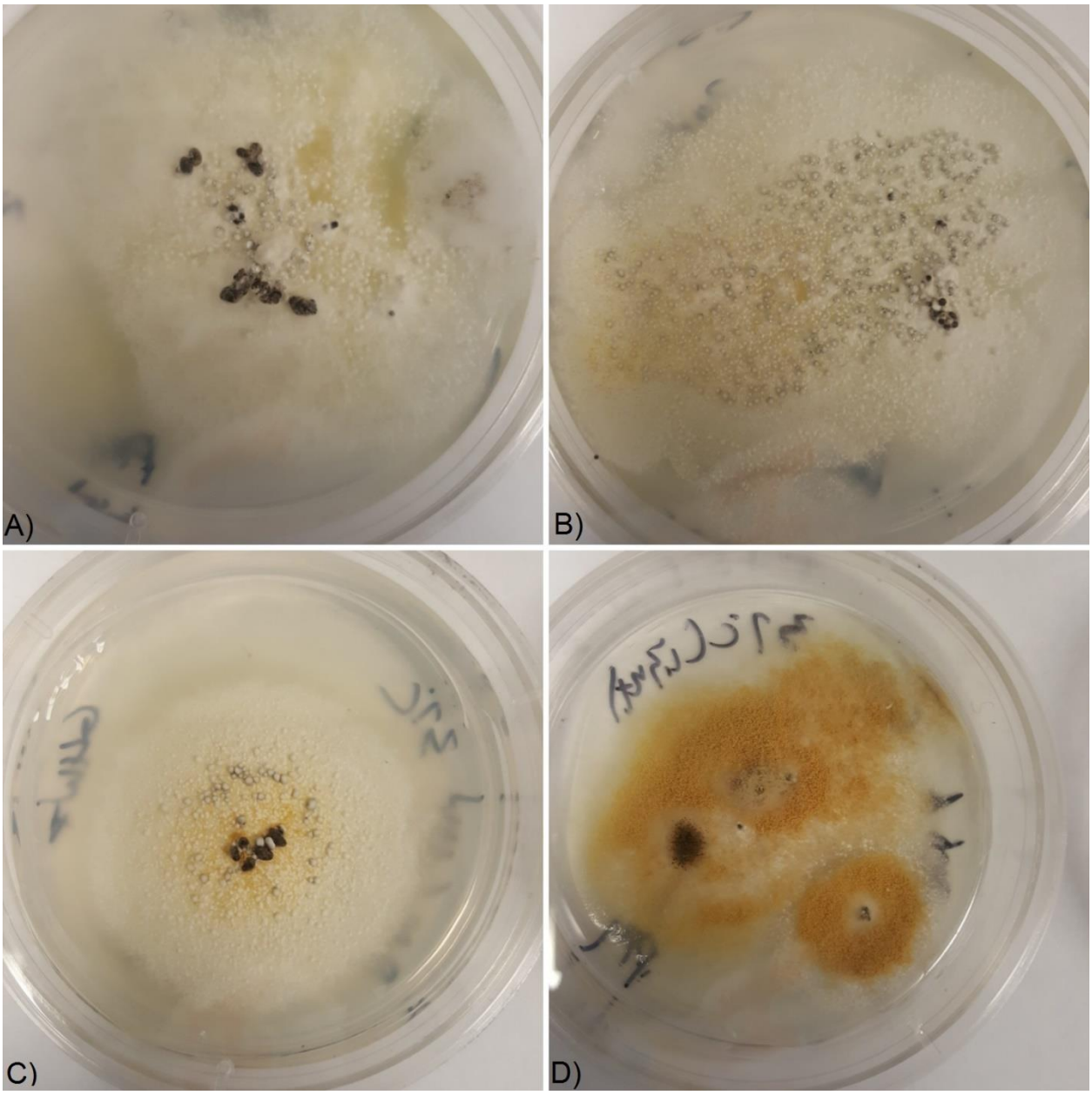

Figure S48: Sclerotia-forming *A. alliaceus* phenotype study on Czapek-Dox agar under A) no light, 25°C, B) light, 25°C, C) no light, 37°C and D) light, 37°C with pictures taken between five and seven days of growth.

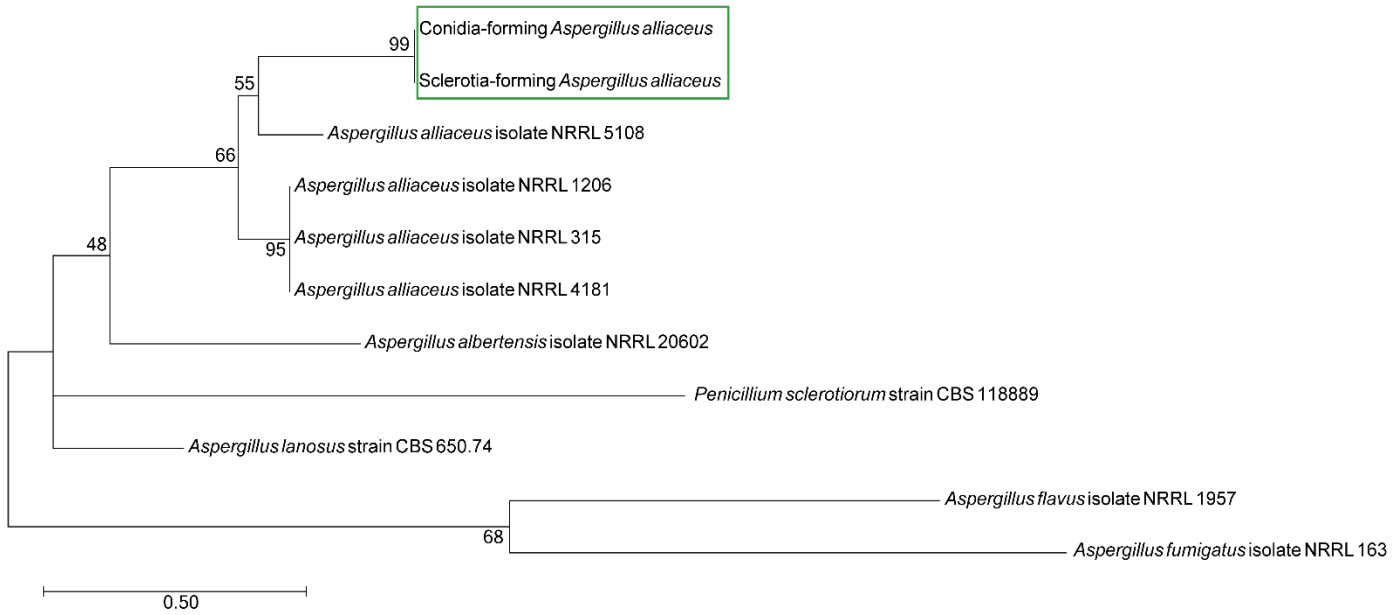

Figure S49: Molecular phylogenetic analysis of the total loci (Beta-Tubulin Bt2a/Bt2b, Calmodulin CF1M/ CF4, and Internal Transcribed Spacer ITS5/4 and ITS1/4) of the *Aspergillus alliaceus* phenotypes by Maximum Likelihood method. The evolutionary history was inferred by using the Maximum Likelihood method based on the Tamura-Nei model.[1] The tree with the highest log likelihood (-11779.1611) is shown. The percentage of trees in which the associated taxa clustered together is shown next to the branches. Initial tree(s) for the heuristic search were obtained automatically by applying Neighbor-Join and BioNJ algorithms to a matrix of pairwise distances estimated using the Maximum Composite Likelihood (MCL) approach, and then selecting the topology with superior log likelihood value. The tree is drawn to scale, with branch lengths measured in the number of substitutions per site. The analysis involved 11 nucleotide sequences. All positions with less than 95% site coverage were eliminated. That is, fewer than 5% alignment gaps, missing data, and ambiguous bases were allowed at any position. There were a total of 1243 positions in the final dataset. Evolutionary analyses were conducted in MEGA7.[2] *A. alliaceus* strains NRRL 315, 5108, and 4181 are referred to as the *Petromyces alliaceus*[3] and *A. alliaceus* strain NRRL 1206 is referred to as *Aspergillus alliaceus*[4].

GATCCCTACCGA-
TGCATGGGATCTAATGCGTCCCATTACTTCTGCCACGTGTTTGCTAACGGTTTTACAGGCAGA
CCATTTCTGGCGAGCACGGCCTTGACGGCTCCGGTGTGTAAGTACAACCCGTGTACA--
TCTCGAACGAAGGACAATCCGTTGG-CGATGGAAGGGTCTGAAAGGG-
TCTGACGGGAAGGATAGTTACAATGGCTCCTCCGACCTCCAGCTGGAGCGCATGAACGTCTA
CTTCAACGAGGTGCGTACCTCAGATTTTGCAGCCTCCCTAGAAACGCCGTGCAGGCCCTGAC
C—
ACTTCTCCAGGCTAGTGGAAACAAGTATGTTCCTCGTGCCGTCCTCGTCGATCTTGAGCCCG
GTACCATGGACGCCGTCCGCGCAGGTCCCTTANGTCAGCTTTTCCGTCCCGACAACTTCGTTG
ATGGTCTTGGTGGAATGCATACTGACTTGAGTTTTCTTGGGCTCCTAATAGGACAAGGATGG
TGATGGTTAGTACATCATGTTCCATAAAACCCCCCTTCTAGTGCGACCGACAGTTTTCAGCCG
CTATAATCGTCTCCATATTTTTTATTGTTCGATCGGCTGAAGTCTTGGCGTTGATAAATTGAC
TCGATATGCAGGCCAGATCACCACCAAGGAGTTGGGCACTGTGATGCGCTCTCTGGGCCAGA
ACCCTTCTGAGTCGGAACTCCAGGATATGATCAACGAGGTTGATGCCGATAACAATGGCACC
ATCGACTTCCCTGGTACGCGAGGGCTTTCCTACGGCTCACAGACAAAGAAATTCTATTAACG
TTCGATTAGAGTTCCTTACGATGATGGCCAGAAAGATGAAGGATACCGACTCTGAGGAGGA
GATCCGGGAGGCTTTCAAGGTTTTCGACCGTGATAACAACGGCTTTATCTCCGCCGCGGAGC
TGCGCCACGTCATGACCTCCATCGGTGAGAAACTTACCGATGATGAAGTTGATGAGATGATC
CGCGAGGCGGATCAGGACGGTGATGGCCGGATCGATTGTACGTTGAGAACAACTCCCCATTT
CTTTTACCCGCTGAGGATGAATGTGGATGTGAACCAACCTCCCACCCGTGTATACTGTACCTT
CGTTGCTTCGGCGGGCCCGCCGTCATGGCCGCCGGGGGGCTTCTGCCCC-
CGGGCCCGCGCCCGCCGGAGACACATGAACTCTGTCTG-ATGTAGTGAAGTCTGAGTTG-
ATTGTCACACAATCAGTTAAAACTTTCA----
ACAATGGATCTCTTGGTTCCGGCATCGATGAAGAACGCAGCGAAATGCGATAACTAATGTG
AATTGCAGAATTCCGTGAATCATCGAGTCTTTGAACGCACATTGCGCCCCCTGGTATTCCGG
GGGGCATGCCTGTCCGAGCGTCATTGCTGCCCATCAAGCACGGCTTGTGTGTTGGGTCCTCG
TCCCCCCCCGGGGG-ACGTGCCCGAAAGGCAGCGGCGGCACCGCGTCCG-
GTCCTCGAGCGTATGGGGCTTTGTCACCCGCTCTGCAGGCCCGGCCGGCGCTGGCCGACGCG
AAAG

Figure S50: Conidia-forming *Aspergillus alliaceus* consensus sequence (1545 bp) of Beta-tubulins (black letters), Calmodulin (blue letters), and ITS region (green letters)

GATCCCTACCGA-
TGCATGGGATCTAATGCGTCCCATTACTTCTGCCACGTGTTTGCTAACGGTTTTACAGGCAGA
CCATTTCTGGCGAGCACGGCCTTGACGGCTCCGGTGTGTAAGTACAACCCGTGTACA--
TCTCGAACGAAGGACAATCCGTTGG-CGATGGAAGGGTCTGAAAGGG-
TCTGACGGGAAGGATAGTTACAATGGCTCCTCCGACCTCCAGCTGGAGCGCATGAACGTCTA
CTTCAACGAGGTGCGTACCTCAGATTTTGCAGCCTCCCTAGAAACGCCGTGCAGGCCCTGAC
C—
ACTTCTCCAGGCTAGTGGAAACAAGTATGTTCCTCGTGCCGTCCTCGTCGATCTTGAGCCCG
GTACCATGGACGCCGTCCGCGCAGGTCCCTTCGGTCAGCTTTTCCGTCCCGACAACTTCGTTG
ATGGTCTTGGTGGAATGCATACTGACTTGAGTTTTCTTGGGCTCCTAATAGGACAAGGATGG
TGATGGTTAGTACATCATGTTCCATAAAACCCCCCTTCTAGTGCGACCGACAGTTTTCAGCCG
CTATAATCGTCTCCATATTTTTTATTGTTCGATCGGCTGAAGTCTTGGCGTTGATAAATTGAC
TCGATATGCAGGCCAGATCACCACCAAGGAGTTGGGCACTGTGATGCGCTCTCTGGGCCAGA
ACCCTTCTGAGTCGGAACTCCAGGATATGATCAACGAGGTTGATGCCGATAACAATGGCACC
ATCGACTTCCCTGGTACGCGAGGGCTTTCCTACGGCTCACAGACAAAGAAATTCTATTAACG
TTCGATTAGAGTTCCTTACGATGATGGCCAGAAAGATGAAGGATACCGACTCTGAGGAGGA
GATCCGGGAGGCTTTCAAGGTTTTCGACCGTGATAACAACGGCTTTATCTCCGCCGCGGAGC
TGCGCCACGTCATGACCTCCATCGGTGAGAAACTTACCGATGATGAAGTTGATGAGATGATC
CGCGAGGCGGATCAGGACGGTGATGGCCGGATCGATTGTACGTTGAGAACAACTCCCCATTT
CTTTTACCCGCTGAGGATGAATGTGGATGTGAACCAACCTCCCACCCGTGTATACTGTACCTT
CGTTGCTTCGGCGGGCCCGCCGTCATGGCCGCCGGGGGGCTTCTGCCCC-
CGGGCCCGCGCCCGCCGGAGACACATGAACTCTGTCTG-ATGTAGTGAAGTCTGAGTTG-
ATTGTCACACAATCAGTTAAAACTTTCA----
ACAATGGATCTCTTGGTTCCGGCATCGATGAAGAACGCAGCGAAATGCGATAACTAATGTG
AATTGCAGAATTCCGTGAATCATCGAGTCTTTGAACGCACATTGCGCCCCCTGGTATTCCGG
GGGGCATGCCTGTCCGAGCGTCATTGCTGCCCATCAAGCACGGCTTGTGTGTTGGGTCCTCG
TCCCCCCCCGGGGG-ACGTGCCCGAAAGGCAGCGGCGGCACCGCGTCCG-
GTCCTCGAGCGTATGGGGCTTTGTCACCCGCTCTGCAGGCCCGGCCGGCGCTGGCCGACGCG
AAAG

Figure S51: Sclerotia-forming *Aspergillus alliaceus* consensus sequence (1545 bp) of Beta-tubulins (black letters), Calmodulin (blue letters), and ITS region (green letters)

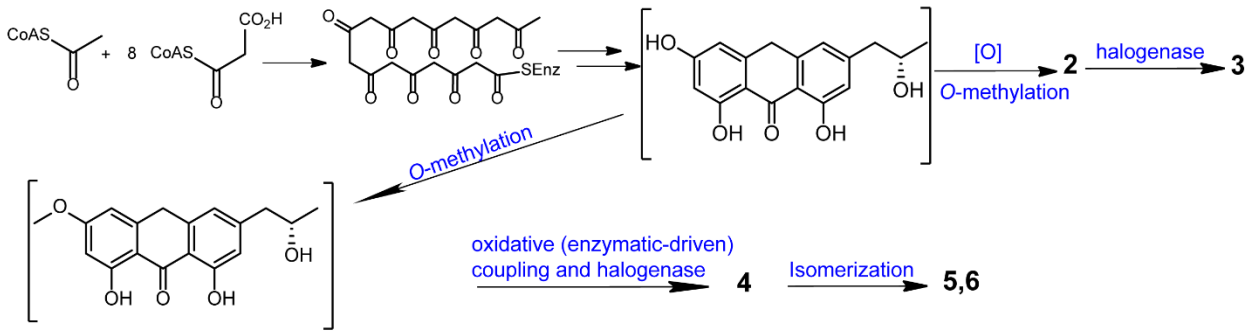

Figure S52. Abbreviated biosynthetic proposal of compounds **2-6**.

References

(1) Tamura, K.; Nei, M. *Mol. Biol. Evol.* **1993**, *10*, 512.

(2) Kumar, S.; Stecher, G.; Tamura, K. *Mol. Biol. Evol.* **2016**.

(3) McAlpin, C.; Wicklow, D. *Can. J. Microbiol.* **2005**, *51*, 1039-1044.

(4) Peterson, S.W. *Mycologia* **2008**, *100*, 205-226.